Geochemistry, diagenesis and mineral associations of laterite deposits along the contact zone of Precambrian basement rocks and Nubia Sandstone between Wadi Dungash and Wadi Shait, South Eastern Desert, Egypt

Ibrahim Abu El-Leil[1], Hatem M. El-Desoky[2] and Ezzat, A. Shafea[3]

[1] Geology Department, Faculty of Science, Al-Azhar University, PO Box 11884, Nasr City, Cairo, Egypt
[2]Geology Department, Faculty of Science, Al-Azhar University, Egypt
[3]Mineral Resources Authority (Egyptian Geological Survey), Egypt

ezzatshafeh@yahoo.com

Abstract: Concentration of SiO_2, Al_2O_3, F_2O_3, Na_2O and K_2O represent the main restricted factors of laterite occurrence. Distribution of these oxides proved that the investigated laterite had formed in the upland area, predominantly of residual origin, under directly weathering of the parent rock into aluminum and iron by very intense leaching of alkalis and silica. Calculation of CIA, ICV, PIA and CIV indices proved that the investigated laterite had been formed by chemical weathering action of Natash Volcanics and decomposition of mafic minerals, accompanied with increasing of clay minerals, leaching of alkalis and increasing of Al^{+3} and Fe^{+3} contents. Mineral associations revealed that the ferruginous rocks often associated with gold, nickel, copper, pyrite and bismuth. Both mottled and ferruginous rocks are associated with Zincite, cerussite, siderite and corundum, to indices their own relationship with laterite occurrence.

[Ibrahim Abu El-Leil, Hatem M. El-Desoky and Ezzat, A. Shafea. **Geochemistry, diagenesis and mineral associations of laterite deposits along the contact zone of Precambrian basement rocks and Nubia Sandstone between Wadi Dungash and Wadi Shait, South Eastern Desert, Egypt.** *J Am Sci* 2017;13(8):32-54]. ISSN 1545-1003 (print); ISSN 2375-7264 (online). http://www.jofamericanscience.org. 5. doi:10.7537/marsjas130817.05.

Keywords: laterite, soil, geochemistry, Eastern Desert, Egypt.

1. Introduction

This paper deals mainly with the geochemistry, diagenesis and mineral association of the investigated laterite and related rocks. According to the prepared geologic map (Fig.1), the investigated laterite deposits comprise the following rock units:

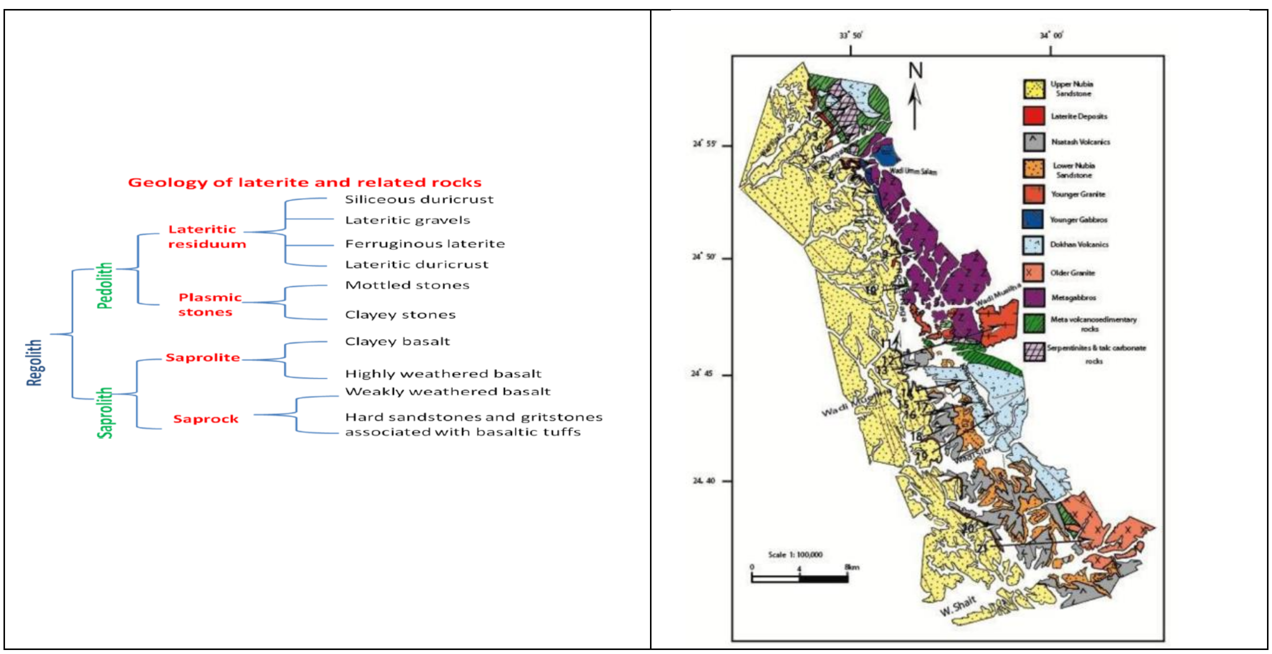

Fig.1. Geological map of the studied district from Wadi Dungash to Wadi Shait

Exactly (67) representative samples had been analyzed for major and trace elements (Tables 1-24). The analyses had been done in the central laboratories of Egyptian Geological Survey. Actually (13) samples are analyzed for weakly weathered basalt, (12) samples from highly weathered basalt, (7) samples from clayey basalt, (6) samples from clay deposits, (9) samples from mottled rocks, (7) samples from lateritic duricrust, (7) samples from ferruginous rocks, and 6 samples from siliceous duricrust.

2. Geochemistry

2.1. Distribution of major elements

According to data given chemical analysis (Tables 1-24), the investigated SiO_2 shows a quite variation in allover the investigated rock units. The high SiO_2 value is recorded in the siliceous duricrust, that reaches (80. 83%) in average, whereas the lower value is recorded in the ferruginous rocks (26.75% in average). On the other hand, SiO_2 content is varying from (36.03% to 59.13%) in the weakly weathered basalt, from (25.8% to59.26%) in the clayey basalt, from (48.6% to 59.62%) in the clay deposits, from (19.58% to 39.82%) in the mottled rocks, from (41.7% to 53.67%) in the lateritic duricrust from (15.05% to 47.37%) in the ferruginous rocks and from (75.62% to 91.75%) in the siliceous duricrust.

Data given clearly show that the low SiO_2 content is recorded in the mottled and ferruginous rocks while the high content is recorded in the siliceous duricrust, the other types have moderate contents. However, it is clear that SiO_2 concentration depends essentially upon the rock source type. Actually, the lower SiO_2 concentration is mainly concentrated at the western part of the area mainly covered by laterite rocks. On the other hand, the eastern part, of the higher SiO_2 content is covered by Nubia Sandstone and Precambrian basement rocks.

Al_2O_3 shows a considerable variation in the investigated laterite and related rocks. Actually, the high Al_2O_3 content is recorded in the mottled and ferruginous rocks reaching up to (29% and 21.04%) respectively. However, the low content is recorded in the siliceous duricrust (7.34%) and weakly weathered basalt (10.94%). The moderate content is recorded in the other rock types. However, it is varying from (12.49%) in the highly weathered basalt to (16.19%) in the claystone.

Tables 1-3. Show major oxides and elements of the saprock

Table 1

	The major oxide of saprock										
	SiO_2	TiO_2	Al_2O_3	Fe_2O_3	MnO	MgO	CaO	Na_2O	K_2O	P_2O_5	L.OI
1-9	50.57	3.76	10.82	15.62	0.42	3.55	7.27	1.75	0.97	1.17	3.69
2-5	44.75	3.71	10.6	14.69	0.67	7.21	9.29	1.56	0.69	0.95	5.32
5-2	46.01	3.91	11.99	16.11	0.24	5.32	9.35	2.69	1.12	1.11	1.86
7-5	40.18	3.34	10.63	14.05	0.79	4.24	14.12	1.82	1.2	0.69	9.63
9-6	49.39	2.96	12.15	14.05	0.52	5.11	9.11	1.76	0.78	0.43	3.27
13-8	49.15	4.07	11.62	11.27	0.26	3.88	8.63	4.9	0.24	0.72	4.97
14-6	47.62	3.37	12.63	14.54	0.21	5.64	9.92	2.96	1.2	0.64	0.99
15-3	52.81	4.95	10.99	6.4	0.24	0.57	11.83	5.44	0.31	0.89	5.28
18-6	42.99	2.3	14.28	7.28	0.93	7.38	6.54	6.77	0.38	0.43	10.03
19-5	37.33	3.87	9.46	12.28	1.49	4.03	16.19	3.03	0.01	1.32	10.70
20-5	36.03	2.86	8.18	14.53	1.23	4.06	17.19	2	0.06	0.33	13.20
21-6	59.12	3.2	11.55	9.55	1.22	1.33	9.55	2.34	0.54	0.3	7.66
21-7	50.26	0.9	7.39	7.27	0	5.66	3.4	2.32	5.64	0	8.81
Aver.	46.63	3.32	10.94	12.12	0.63	4.46	10.18	3.02	1.01	0.74	6.57

Table 2

	The trace elements of saprock								
	Sr	Ga	Ba	Rb	Ta	Zr	Th	Nb	Hf
1-9	457.6	0	355	11.7	2.6	167.3	2.3	31	5.7
2-5	518.1	0	2677.5	19.6	0	247.2	0	31.1	0
5-2	88.3	0	305.7	3.1	0	125.3	0	19.9	0
7-5	322.4	0	95.5	2.3	0	33.4	0	5.5	0
9-6	417.3	0	285	10.1	1.9	129.9	4.3	23.2	5.5
13-8	282.2	0	520.4	4.4	0	267.7	0	35.4	0
14-6	612.3	0	621.1	21.3	0	282.9	0	34.3	0
15-3	652	26	517.4	47.7	0	304	0	36.3	0
18-6	228	0	237.1	8.4	0	553.5	0	98.5	0
19-5	184.7	0	511.4	3.7	0	238.3	0	36.4	0
20-5	191.6	0	1209.6	6.6	0	146.6	0	23.8	0
21-6	105	0	295	8.9	0	1065	0	120	0
21-7	0	0	0	0	0	0	0	0	0
Aver.	312	2	586	11.3	0.3	273	0.5	38.1	0.8

Table 3

	Follow the trace elements of saprock								
	Y	**Cr**	**Pb**	**Ni**	**V**	**Zn**	**Co**	**Cu**	**Mo**
1-9	17.4	29.5	7.6	2.3	395	311.1	53.2	26.7	2.3
2-5	23.3	55.8	26	20.9	253.7	117.1	56.2	32.7	0
5-2	6.2	103.5	4.1	44	186.5	222.4	122.9	31.7	0
7-5	2	1033.8	3	306.3	112.9	50.5	44.2	9.5	0
9-6	15.6	45.7	10	2.3	365	109.6	35.2	1.5	1.5
13-8	16.3	248.6	6.2	76.3	262.4	172	33.8	93	0
14-6	18.3	189.7	2.2	49.6	246.8	102.3	52	55.8	0
15-3	39	38.3	4.7	32.2	287.2	86	77.1	8.7	0
18-6	44.7	33.6	11.6	42.1	404.8	295.8	79.6	51.4	0
19-5	36.4	28.6	3	9.7	279.7	123	46.3	211.3	0
20-5	12.7	211.3	2.1	68.7	276.9	129.8	81.7	91.4	0
21-6	52	31	15	45	320	124	93	6	0
21-7	0	0	0	0	0	0	0	0	0
Aver.	21	157	7.3	53	260	141	59.6	55.7	0.29

Tables 4-6. Show major oxides and elements of the saprolite (Highly weathered basalt)

Table 4

	The major oxide saprolite									
	SiO_2	**TiO_2**	**Al_2O_3**	**Fe_2O_3**	**MnO**	**MgO**	**CaO**	**Na_2O**	**K_2O**	**P_2O_5**	**L.OI**
1-8	48.99	4.03	12.17	14.87	1.21	3.76	6	1.41	0.46	0.82	5.88
6-3	47.11	4.93	10.93	13.42	0.93	3.11	8.14	2.95	0.06	1.14	6.88
6-7	49.75	4.08	11.1	14.57	0.37	3.98	8.48	2.36	1.05	1.23	2.62
10-8	48.45	2.91	13.45	14.13	0.59	6.26	6.53	2.38	0.67	0.42	3.82
11-2	43.23	2.9	14.5	21.7	0.2	0.75	4.9	4.4	0.33	0.78	5.5
12-7	47.49	4.95	11.16	16.09	0.32	7.66	2.54	3.5	0.01	0.4	4.58
12-8	54.18	3.84	14.34	11.06	0.09	0.99	5.1	6.2	0.77	0.72	1.9
14-4	43.54	3.8	10.23	15.95	0.12	3.51	6.06	2.69	1.29	0.82	10.92
14-3	37.6	3.87	10.59	15.13	0.12	3.4	3.01	0.93	0.44	0.52	15.72
14-2	48.17	4.1	11.28	15.89	0.41	5.4	6.43	2.91	0.22	0.88	4.10
16-7	44.17	2.82	15.53	11.64	0.59	4.93	9.17	2.47	0.68	0.51	7.19
17-8	44.34	2.64	14.64	15.36	0.51	3.67	9.98	2.74	0.33	0.49	5.99
Aver.	46.34	3.7	12.49	14.98	0.45	3.95	6.36	2.91	0.52	0.72	6.25

Table 5

	The trace elements of saprolite								
	Sr	**Ga**	**Ba**	**Rb**	**Ta**	**Zr**	**Th**	**Nb**	**Hf**
1-8	336.1	0	912	10.3	0.7	173.8	2.2	35.1	1.2
6-3	235.9	0	745	2.8	3.2	175.7	3.8	38.3	4.9
6-7	469.8	0	325	11.8	2.1	175.1	1.9	32.5	5.7
10-8	411.8	0	243.5	10.6	1.8	138.6	4.7	23.2	2.6
11-2	0	0	0	0	0	0	0	0	0
12-7	0	0	0	0	0	0	0	0	0
12-8	402.6	0	697.3	8.3	0	268.7	0	31	0
14-4	110	0	198.8	5.8	0	919.6	0	40.2	0
14-3	0	0	0	0	0	0	0	0	0
14-2	367.4	0	582.3	3.8	0	252.1	0	31.6	0
16-7	516.1	0	777.4	15.2	0	215	0	27	0
17-8	478.2	0	463.5	7.7	0	201.1	0	25.6	0
Aver.	277.3	0	412	6.35	0.6	210	1.0	23.7	1.2

Table 6

	Follow the trace elements of saprolite								
	Y	Cr	Pb	Ni	V	Zn	Co	Cu	Mo
1-8	19.5	24.9	5.8	9.6	411	1149.3	152	205.4	1.6
6-3	17.8	55.2	6.8	2.3	504	78.1	63.9	35.5	1.5
6-7	18.8	31.2	6.3	2.8	413	67.3	42.7	18.5	1.5
10-8	15.6	61.1	5	8	375	57.1	46.5	66.2	1.5
11-2	0	0	0	0	0	0	0	0	0
12-7	0	0	0	0	0	0	0	0	0
12-8	11.5	172.2	22	28.1	219.6	48.5	27.9	9.5	0
14-4	24.6	32	3.3	21.7	321.7	122.9	54.7	36.7	0
14-3	0	0	0	0	0	0	0	0	0
14-2	15.4	42.7	1.7	40.9	300.3	165.5	61	21.6	0
16-7	12.4	175	2.6	31.7	289.9	69.3	66.3	15.7	0
17-8	0	0	0	0	0	0	0	0	0
Aver.	11	49.5	4.4	12	236	147	42.9	34	0.5

Tables7-9. Show major oxides and elements of the saprolite (clayey basalt)

Table 7

	The Major Oxide of Saprolite										
	SiO_2	**TiO_2**	**Al_2O_3**	**Fe_2O_3**	**MnO**	**MgO**	**CaO**	**Na_2O**	**K_2O**	**P_2O_5**	**L.OI**
1-7	46.02	3.29	15.74	13.54	0.88	6.1	5.15	2.02	0.35	0.97	5.60
6-1	52.99	3.16	14.01	15.46	0.07	1.47	2.79	0.8	1.75	0.41	6.68
12-6	40.25	2.36	15.95	10.04	0.04	2.03	2.93	7.05	0.88	0.82	8.38
15-2	37.95	3.08	15.6	16.71	0.11	2.12	5.59	5.68	1.57	0.53	10.57
18-2	59.26	1.61	16.11	5.68	0.03	3.46	1.24	2.2	2.51	0.1	5.91
18-4	55.01	1.56	14.3	6.66	0.06	3.8	4.63	1.95	2.14	0.2	5.31
20-4	25.8	2.76	16.5	16	0.08	1.26	1.26	13.55	0.12	0.14	10.7
Aver.	45.3	2.54	15.45	12.01	0.18	2.89	3.37	4.75	1.33	0.45	7.59

Table 8

	The trace elements of Saprolite								
	Sr	**Ga**	**Ba**	**Rb**	**Ta**	**Zr**	**Th**	**Nb**	**Hf**
1-7	331.7	22.1	1067.1	14.1	0	248.5	0	33.6	0
6-1	305.2	0	29.1	38.4	2.8	326.8	7.1	88.1	9.1
12-6	395.5	0	303.2	7	0	1577.4	0	144.9	0
15-2	234.7	0	694.8	5	0	241.9	0	32.1	0
18-2	102	0	205.7	6.6	0	1871.8	0	50.8	0
18-4	116	0	378.4	10.1	0	1200.5	0	91.3	0
20-4	160	0	249.6	11	0	745.8	0	128.9	0
Aver.	235	3.1	418	13	0.4	887	1	81.3	1.3

Table 9

	The trace elements of Saprolite								
	Y	Cr	Pb	Ni	V	Zn	Co	Cu	Mo
1-7	25.3	28.7	3.6	55.3	268	988.6	179.4	190.8	0
6-1	28.5	63.1	12.6	2.4	304	55.7	36	1.5	1.8
12-6	98.9	46.6	18.5	81.2	303.4	84.8	72.2	11.6	0
15-2	21.2	80.6	4.6	16.6	263.3	50.1	16.5	566.4	0
18-2	29.1	26.2	20.3	34.4	207.7	92.1	49.7	113.3	0
18-4	54.4	22.5	19	47.9	215.1	106	46.8	21.2	0
20-4	62.7	117.8	16.1	46.5	513.2	43.8	91.8	9.7	0
Aver.	45.7	55.07	13.5	40.6	296	203	70.3	130	0.2

Tables 10-12. Show major oxides and elements of the claystones

Table 10

	The Major Oxide of claystones										
	SiO_2	**TiO_2**	**Al_2O_3**	**Fe_2O_3**	**MnO**	**MgO**	**CaO**	**Na_2O**	**K_2O**	**P_2O_5**	**L.OI**
6-4	57.41	2.71	14.3	9.7	0.04	1.89	3.49	0.92	2.04	0.58	6.50
9-5	56.93	2.54	18.43	13.04	0.04	0.27	1.2	0	1.05	0.23	5.98
13-5	48.48	1.25	14.36	7.62	0.01	0.62	1.5	7.84	0.11	0.5	8.32
13-6	48.6	1.21	17.32	4.62	0.01	0.67	1.61	6.56	0.16	0.14	8.76
18-5	59.62	1.7	16.22	5.63	0.02	3.66	1.2	2.1	2.56	0.3	5.54
21-4	54.11	2.53	16.55	10.11	0.05	2.75	1.33	2.77	1.33	0.4	6.35
Aver.	54.19	1.99	16.19	8.45	0.02	1.64	1.72	3.36	1.20	0.35	6.90

Table 11

	The trace elements of claystones								
	Sr	**Ga**	**Ba**	**Rb**	**Ta**	**Zr**	**Th**	**Nb**	**Hf**
6-4	266.4	0	475	50.2	1.3	381.5	3.4	99.3	7.2
9-5	521.9	0	845	30.7	1.6	449.4	10.1	84.7	11.1
13-5	110	0	198.8	5.8	0	919.6	0	40.2	0
13-6	160	0	205.7	6.6	0	174.5	0	50.8	0
18-5	105	0	230.7	11.3	0	1872.1	0	93.4	0
21-4	98	0	308.6	7.7	0	1070.8	0	134	0
Aver.	210	0	391	18.7	0.4	811	2.2	83.7	3

Table 12

	Follow the trace elements of claystones								
	Y	Cr	Pb	Ni	V	Zn	Co	Cu	Mo
6-4	36.7	49.8	8.7	2.5	255	78.9	29.5	42.8	2.8
9-5	59.6	45.8	10.7	2	250	32.7	32.5	1.5	2.4
13-5	59.6	45.8	10.7	2	250	32.7	32.5	1.5	2.4
13-6	18.8	69.8	26.9	31.5	364.4	19.1	65.5	18.9	0
18-5	52	24.9	21.5	35	222.2	90	52	114.9	0
21-4	44.6	36.6	12.6	57.3	307.2	101.3	107.6	7.3	0
Aver.	45.2	45.4	15.1	21.7	275	59.1	53.2	31.1	1.2

Tables 13-15. Show major oxides and elements of the mottled rocks

Table 13

	The Major Oxide of mottled rocks										
	SiO_2	**TiO_2**	**Al_2O_3**	**Fe_2O_3**	**MnO**	**MgO**	**CaO**	**Na_2O**	**K_2O**	**P_2O_5**	**L.OI**
2-4	38.86	4.6	21.5	22.36	0.11	1.64	0.99	0.05	0.99	0.21	8.65
4-6	19.58	3.86	25.52	39.94	0.08	0.73	0.26	0.2	0.01	0.06	9.11
4-7	21.15	3.71	52.92	37.91	0.09	0.04	0.85	0.14	0.03	0.01	8.78
4-8	22.9	4.6	29.1	31.22	0.1	0.9	0.59	0.13	0.07	0	9.18
4-9	21.48	5.32	27.97	30.83	0.09	1.07	0.95	0.8	0.03	0	10.82
4-10	21.5	6.35	28.09	31.98	0.12	0.86	0.55	0.22	0.01	0	9.34
7-2	39	4.13	23.55	20.46	0.07	0.54	1.11	0.37	0.54	0.32	9.59
7-3	37.37	3.2	26.52	20.53	0.06	0.85	0.92	0.12	0.14	0.01	9.63
8-2	39.82	3.28	25.93	21.5	0.09	0.19	0.44	0.01	0.04	0.1	8.44
Aver.	29	4.3	29	28.5	0.09	0.75	0.74	0.22	0.2	0.07	9.28

Table 14

	The trace elements of the mottled rocks								
	Sr	**Ga**	**Ba**	**Rb**	**Ta**	**Zr**	**Th**	**Nb**	**Hf**
2-4	451.9	35.9	1031.5	24.3	0	533.9	0	68.4	0
4-6	503.7	0	595	1.8	3.2	165.2	4.6	30.4	5.9
4-7	271.4	0	255	2.3	2	153.2	3	29.8	6.2
4-8	255.6	0	215	2.6	3.5	197.9	4.6	40.9	6.5
4-9	434.2	0	455	2.2	1.7	237.1	3	48.2	7.4
4-10	293.7	0	243	2.6	2.3	251.2	5.9	54.6	7.7
7-2	288.6	34.8	604.9	15.9	0	351.8	0	45.1	0
7-3	108.2	31.9	499.2	7.6	0	354.8	0	47.6	0
8-2	528.1	24.1	557.9	20.4	0	256.2	0	31.5	0
Aver.	348	14	495	8.85	1.4	278	2.3	44	3.7

Table 15

	Follow the trace elements of the mottled rocks								
	Y	Cr	Pb	Ni	V	Zn	Co	Cu	Mo
2-4	127.4	59.5	17.6	101.4	343.3	92.5	113.6	5.4	0
4-6	7.8	242.3	15.9	2.5	801	9.7	97.2	1	1.5
4-7	8.5	119.4	14.6	3.1	855	8.7	75.5	1.5	1.5
4-8	8.4	134.2	13.9	2.5	875	16.7	72	1.5	1.5
4-9	9.5	210.8	15.2	2.6	887	18.8	80.1	1.5	1.9
4-10	9.6	70.6	15.4	2.5	1115	25.9	85.6	1.5	1.5
7-2	40.4	51.2	15.5	42.4	465.9	61.5	88.7	5.3	0
7-3	15.3	17	20.6	42	372.2	103.2	105.4	8.8	0
8-2	21.9	77.3	4.2	25.4	266.2	314.5	84.9	44.5	0
Aver.	27.6	109	14.7	45	664	72.3	29.2	7.88	0.8

Tables 16-18. Show major oxides and elements of the lateritic duricrust rocks

Table 16

	The Major Oxide of lateritic duricrust rocks										
	SiO_2	**TiO_2**	**Al_2O_3**	**Fe_2O_3**	**MnO**	**MgO**	**CaO**	**Na_2O**	**K_2O**	**P_2O_5**	**L.OI**
16-3	42.79	2.1	14.8	13.4	0.05	2.08	1.38	1.39	2.54	0.06	3.44
16-4	53.33	1.72	15.11	6.66	0.04	3.72	1.42	5	2.35	0.05	5.96
16-5	53.67	1.97	18.73	7.3	0.03	4.35	1.3	2.58	3.29	0.09	5.15
16-6	49.53	2.44	17.32	12.01	0.05	3.7	1.4	2.11	2.11	0.09	6.42
17-3	41.7	1.23	18.2	8.76	0.09	3.75	2.14	9.65	2.02	0.3	4.85
17-5	42.88	1.14	12.6	6.36	0.09	3.32	1.44	13.39	2.46	0.42	6.35
19-4	48.82	2.66	16.02	12.64	0.15	3.62	4.12	1.39	1.61	0.86	7.66
Aver.	47.53	1.89	16.11	9.59	0.07	3.50	1.88	5.07	2.34	0.26	5.69

Table 17

	The trace elements of lateritic duricrust rocks								
	Sr	**Ga**	**Ba**	**Rb**	**Ta**	**Zr**	**Th**	**Nb**	**Hf**
16-3	0	0	0	0	0	0	0	0	0
16-4	101	0	378.4	10.1	0	1002.8	0	91.3	0
16-5	78.5	0	230.7	11.3	0	1049.4	0	93.4	0
16-6	134	0	237.1	8.4	0	1075.6	0	98.5	0
17-3	402	0	249.6	11	0	1461.5	0	128.9	0
17-5	77.8	0	480.1	12.1	0	1745.3	0	153	0
19-4	290.4	0	457.6	44.3	0	338.9	0	40.9	0
Aver.	154.8	0	290	13.8	0	953	0	86.5	0

Table 18

	Follow the trace elements of lateritic duricrust rocks								
	Y	Cr	Pb	Ni	V	Zn	Co	Cu	Mo
16-3	0	0	0	0	0	0	0	0	0
16-4	54.4	23.5	20	47.9	236.8	96.7	79.1	38	0
16-5	52	22.9	16.9	35	289.6	108.6	56.6	31.7	0
16-6	44.7	29.7	14.1	42.1	312.4	204.9	83.4	11.4	0
17-3	62.7	24.9	17.8	46.5	202.2	121.1	59	24.4	0
17-5	64.5	22.8	11.4	32.4	212.9	223.3	74.1	37.9	0
19-4	31.8	38.4	4.2	23.4	231.5	121.6	56.1	21.1	0
Aver.	44.3	23.1	12	32.4	212.2	125.1	58.3	23.5	0

Tables 19-.21. Show major oxides and elements of the ferruginous laterite rocks

Table 19

	The major oxide of ferruginous laterite rocks										
	SiO_2	**TiO_2**	**Al_2O_3**	**Fe_2O_3**	**MnO**	**MgO**	**CaO**	**Na_2O**	**K_2O**	**P_2O_5**	**L.OI**
1-4	34.77	5.51	13.38	24.81	0.07	0.36	8.42	0.02	0.07	2.2	8.36
1-5	29.28	3.03	18.81	34.61	0.07	1.74	0.66	0.12	1.1	0.09	10.43
1-6	47.37	4.11	18.85	19.65	0.04	2.32	2.87	0.49	1.47	0.07	7.36
3-7	15.05	3.52	18.01	54.67	0.12	0.45	0.36	0.16	0.04	0	6.97
3-8	22.58	4.37	31.78	30.09	0.07	0.59	0.54	0.09	0.03	0.01	8.96
3-9	18.82	4.67	24	42	0.11	0.55	0.49	0.09	0.01	0.01	8.18
9-3	19.43	6.22	22.51	38.19	0.12	0.73	1.1	0.1	0.02	0.2	9.42
Aver.	26.75	4.49	21.04	34.8	0.08	0.96	2.06	0.15	0.39	0.36	8.52

Table 20

	The trace elements of ferruginous laterite rocks								
	Sr	**Ga**	**Ba**	**Rb**	**Ta**	**Zr**	**Th**	**Nb**	**Hf**
1-4	266.4	0	103	4.3	1.3	173.5	1.7	40.9	5.8
1-5	243	32.8	450.9	6	0	349.7	0	44.2	0
1-6	225.2	0	115.2	30.6	2	157.1	1.7	34.1	5.2
3-7	208.2	0	289	1.8	1.8	116.8	2.8	23.9	4.4
3-8	316.6	0	802	1.3	2.9	205.1	2.7	42	7.4
3-9	285.8	0	387	1.6	1.2	230.5	7.6	45.4	8
9-3	278.6	0	565	1.8	3.4	167	5.8	36.5	4.4
Aver.	260	4.68	387	6.77	1.8	200	3.1	38.1	5

Table 21

	The trace elements of ferruginous laterite rocks								
	Y	Cr	Pb	Ni	V	Zn	Co	Cu	Mo
1-4	44.6	48.5	10.8	2.4	701	49.3	74.1	1.5	1.6
1-5	22.6	56.3	10.1	72.9	493.1	149.2	200.3	5.9	0
1-6	28.3	25.3	12.2	34.3	435	63.1	103	1.5	1.6
3-7	7.5	150.6	24.9	2.2	803	7.7	104.2	1.5	1.5
3-8	14.8	107.5	16.7	2.2	825	17.1	64.4	1.5	1.5
3-9	10.2	19.7	25.5	2.3	809	17.6	76.6	1.5	1.6
9-3	17.9	64.6	16.1	2.5	1350	26.7	85	1.5	1.9
Aver.	20.8	67.5	16.6	16.9	773	47.2	101	2.1	1.38

Tables 22-24. Show major oxides and elements of the siliceous duricrust rocks

Table 22

	The major oxide of siliceous duricrust rocks										
	SiO_2	**TiO_2**	**Al_2O_3**	**Fe_2O_3**	**MnO**	**MgO**	**CaO**	**Na_2O**	**K_2O**	**P_2O_5**	**L.OI**
3-5	81.28	0.7	7.73	5.67	0.06	0.05	1.44	0.01	1.22	0.16	1.52
3-6	75.07	1.85	10.36	7.66	0.16	0.01	1.27	0.01	0.76	0.2	2.56
9-1	91.79	0.43	2.87	1.61	0	0.29	1.48	0.01	0.13	0.1	1.08
9-2	78.71	1.24	7.02	7.51	0.07	0.24	1.49	0.4	0.37	0.13	2.42
10-5	80.99	0.93	8.48	3.47	0.02	0.08	0.66	1.45	0.4	0.09	3.04
10-6	77.14	1.43	7.58	7.14	0.16	0.25	0.96	0.83	0.59	0.16	3.37
Aver.	80.83	1.09	7.34	5.51	0.07	0.15	1.21	0.45	0.57	0.14	2.33

Table 23

	The trace elements of siliceous duricrust rocks								
	Sr	**Ga**	**Ba**	**Rb**	**Ta**	**Zr**	**Th**	**Nb**	**Hf**
3-5	55.1	0	556	36.3	1.4	107.3	3.6	18.3	3
3-6	135.8	0	502	23.1	2.9	208.4	6.6	32.3	7.2
9-1	15.8	0	285.5	6.9	2.9	96.2	7.3	12.3	5.4
9-2	157.6	0	345	10.7	5.5	193	7.5	28.6	5
10-5	15.8	0	285.5	6.9	2.9	96.2	7.3	12.3	5.4
10-6	157.6	0	345	10.7	5.5	193	7.5	28.6	5
Aver.	89.6	0	386	15.7	3.5	149	6.63	22.6	5.1

Table 24

	The trace elements of siliceous duricrust rocks								
	Y	Cr	Pb	Ni	V	Zn	Co	Cu	Mo
3-5	15.2	140.2	9.9	2.5	75	10.6	8.2	2.7	1.8
3-6	18.6	218.3	14	2.2	175	14.9	14.8	1.5	2.2
9-1	12	65.3	6.9	25.7	57.4	45.7	141.4	9.7	2.4
9-2	18.5	148.8	13.4	15	106	57.7	18.5	18.9	2.4
10-5	18.5	102	8	4.2	92	25.2	112.4	66.3	2.4
10-6	20.9	324.6	10.3	15.8	162	31.8	77.1	21.8	2
Aver.	17.28	166	10.4	10.9	111	30.9	62	20.1	2.2

Generally, behavior of Al_2O_3 depends essentially upon SiO_2 content. Actually, it is observed that SiO_2 shows reverse relationship with SiO_2, whereas the mottled and the ferruginous rocks of high Al_2O_3content obtaining with low SiO_2 content.

Fe_2O_3 represents the main oxide in the formation of lateritic rocks, beside Al_2O_3. The concentration of Fe_2O_3 is quietly coinciding with Al_2O_3 content. However, the mottled and ferruginous rocks of high Al_2O_3 have higher Fe_2O_3 content. Actually, average content reaches (28.5%) in the mottled rocks and (34.8%) in the ferruginous rocks. The lowest content (5.51%) is recorded in the siliceous duricrust, of higher SiO_2 content (80.83%) However, the other rock units have moderate contents, varying from (8.45%) in the claystone to (14.98%) in the highly weathered basalt (Tables 25).

Calculation of (Al_2O_3+Fe_2O_3) content shows that the higher value is connected within the mottled rocks, with the average up to (57.5%), as well as the ferruginous rocks up to (55.84%), (Tables 26). The lowest value that reaches (12.86%) is for the siliceous duricrust rocks. However, the values for other rocks are varying from (26.6%) in the weakly basalt to (27.47%) in the highly weathered basalt (Fig.2).

Al_2O_3/Fe_2O_3 ratios are also calculated (Table 26 & Fig.4) to show Al_2O_3 content relative to Fe_2O_3. The given results demonstrate that mottled rocks have Al_2O_3/ Fe_2O_3 ratio up to (1.02), whereas it becomes (0.6) in the ferruginous rocks. This means that aluminum content exceeding iron content in the mottled rocks and vice versa for the ferruginous rocks. Moreover, aluminum content exceeds iron in the clayey basalt (1.29), claystone (1.92), lateritic duricrust1.68 and siliceous duricrust (1.33). The oxides SiO_2, Fe_2O_3 and Al_2O_3 are used by different authors to classify the laterite and bauxite deposits. According to SiO_2 - Fe_2O_3 - Al_2O_3 ternary diagram of **Dury** 1**969,** the investigated samples are plotted the field of ferruginous siliceous duricrust (Fig.5). However, they are plotted on ferrossialitic field of ternary SiO_2 - Fe_2O_3 - Al_2O_3 diagram of **Dury, 1969 and Mac Farlane, 1983**, (Fig.6).

Both Na_2O and K_2O represent another important factor for concentrations and occurrence of the deposits. Actually, these two oxides show reverse relationship with laterite concentration. However, it is noticed that the lateritic duricrust of higher Na_2O content (5.07%) has lower (Al_2O_3 + Fe_2O_3) content (25.7%). The lowest Na_2O average content (0.15%) is recorded in the ferruginous rocks. In the claystone, it reaches (3.36%). However, it becomes lesser in the siliceous duricrust (0.57%). Moreover, in the highly weathered basalt, it reaches (2.91% and 3.02%) in the weakly weathered basalt (Tables 25 & 26).

Tables 25. Show the average major oxide contents of the different regolith profile units.

	SiO_2	TiO_2	Al_2O_3	Fe_2O_3	MnO	MgO	CaO	Na_2O	K_2O	P_2O_5
Saprock (L.W. Basalt)	46.63	3.32	10.94	12.12	0.63	4.46	10.18	3.02	1.01	0.74
Saprolite (H.W. Basalt)	46.34	**3.7**	12.49	14.98	0.45	3.95	6.36	2.91	0.52	0.72
Saprolite (C. Basalt)	45.3	2.54	15.45	12.01	0.18	2.89	3.37	4.75	1.33	0.45
Claystone	54.19	1.99	16.19	8.45	0.02	1.64	1.72	3.36	1.20	0.35
Mottled rocks	29	4.3	29	28.5	0.09	0.75	0.74	0.22	0.2	0.07
Lateritic duricrust	47.53	1.89	16.11	9.59	0.07	3.50	1.88	5.07	2.34	0.26
Ferruginous laterite	26.75	4.49	21.04	34.8	0.08	0.96	2.06	0.15	0.39	0.36
Siliceous duricrust	80.83	1.09	7.34	5.51	0.07	0.15	1.21	0.45	0.57	0.14

Table 26. The relation of Al_2O_3 & Fe_2O_3 along the weathered cross sections

	$Al_2O_3+Fe_2O_3$	Fe_2O_3/Al_2O_3	Al_2O_3/Fe_2O_3
Saprock (L. W. Basalt)	23.06	1.10	0.90
Saprolith (H. W. Basalt)	27.47	1.12	0.83
Saprolith (Clayey Basalt)	27.46	0.77	1.28
Pedolith (Clay Deposits)	24.64	0.52	1.91
Mottled Zone	57.5	0.98	1.02
Lateritic Duricrust	25.7	0.59	1.68
Ferrug. Zone	55.84	1.65	0.60
Siliceous Duricrust	12.85	0.75	1.33

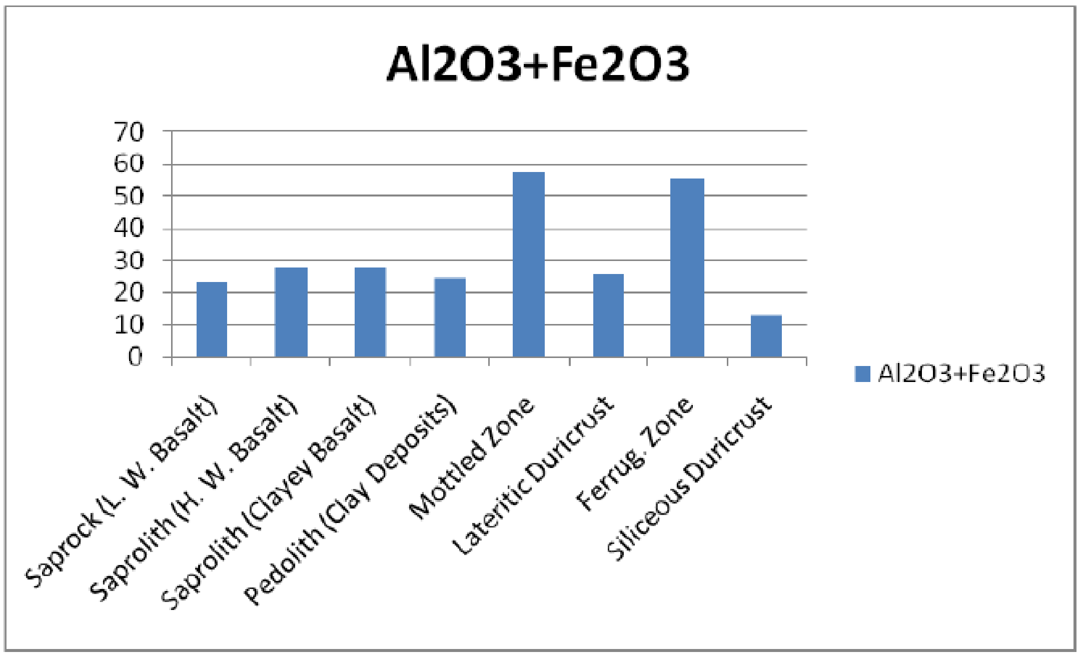

Fig.2. Showing histogram of the calculation Al_2O_3+Fe_2O_3 for different regolith cross-sections.

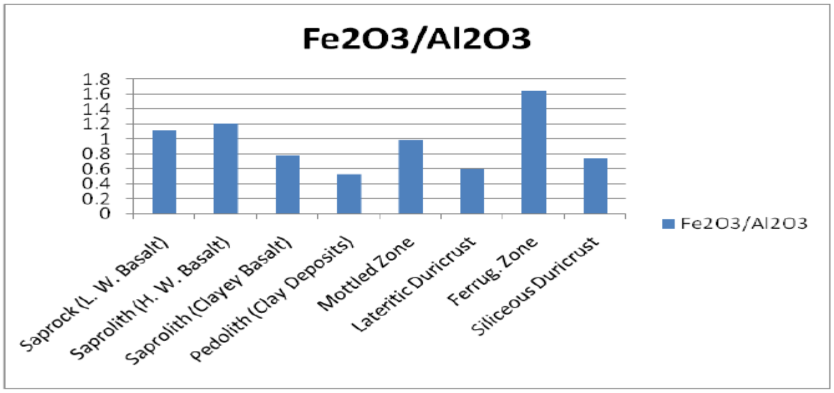

Fig.3. Showing histogram of the calculation Fe_2O_3/ Al_2O_3 for different regolith cross-sections.

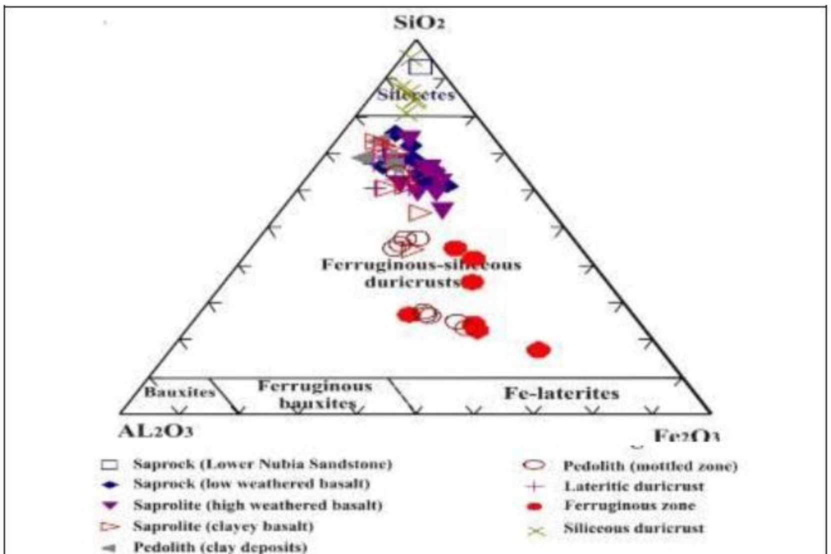

Fig 5. Showing SiO_2- Al_2O_3-Fe_2O_3 ternary digram of the regolith profiles (**Dury, 1969**).

Showing histogram of the calculation Al_2O_3/Fe_2O_3 for different regolith cross sections.

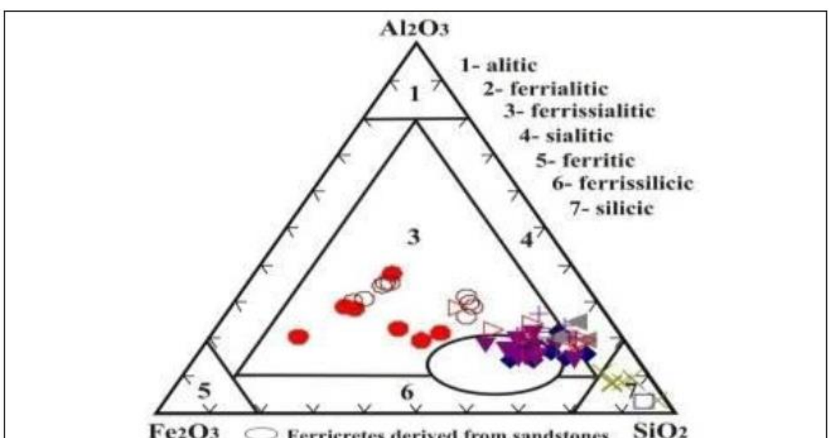

Fig.6. Triangular diagram of ferricrete classification of the studied regolith profile (**Dury, 1969** and **MacFarlane, 1983**). Symbols as in Fig. (5).

K_2O more or less behaviors like Na_2O relative to SiO_2, Al_2O_3 and Fe_2O_3. However, the higher content (3.34%) is recorded within the lateritic duricrust and the lowest 0.2% in the mottled rocks. Moreover, K_2O is varying from 0.57% in the siliceous duricrust and 1.33% in the clayey basalt.

However, the Precambrian basement rocks and siliceous duricrust rocks mainly cover the area of higher concentration. Mottled and ferruginous rocks (Tables 27 & 28) mainly cover the lowest concentrated with K_2O and Na2O. These two oxides (K_2O and Na_2O) are coinciding well with SiO_2, which they show a reverse relationship with Fe_2O_3 and Al_2O_3.

The optimum relationship between the five oxides (SiO_2, Al_2O_3, Fe_2O_3, Na_2O and K_2O) represents the main restricted factors during occurrence and development of the lateritic rocks. The insitue resilicification of the based saprolith zone (weakly and highly weathered basalt) is caused by large amount of the silica free decomposing, by processes of weathering and may be responsible for SiO_2 fixation in the top most zone, leading to clay mineral formation (**Valeton, 1972)** Furthermore, a direct relationship between SiO_2 distribution and intensity of weathering action is also observed, whereas during early stages of diagenesis enrichment of silica is reciprocal of that aluminum.

In the laterite deposits on igneous rocks, silica is highest in the lowest and uppermost zones, (**Valeton, 1972**). This behavior is well observed on the most of the examined cross-sections. An increasing of the weathering action following by increasing spread of SiO_2, removed and increasing relative enrichment of alumina and iron govern the early stages of diagenesis. There is absolute enrichment by iron impregnation of the upper iron crust in many parts of the saprolith. The common primary iron mineral is hematite.

Chemical mineralogical reaction that took place during weathering of rocks into saprolith and pedolith are: **a)** Kaolinitization of alumino-silicate minerals, **b)** Hematization of Fe-bearing minerals, **c)** Formation of hydroxide minerals from kaolinite or directly from feldspar through in congruent dissolution, **d)** Congruent dissolution of kaolinite minerals, **e)** Dissolution of quartz.

Moreover, distribution of these five oxides (SiO_2, Al_2O_3, Fe_2O_3, Na_2O and K_2O) proved that the investigated lateritic rocks had been formed in the upland areas that are predominantly residual in origin formed under free leaching conditions (**Grubb, 1973 and Hutchison, 1983**). However, the minerals of the parent, rock are directly weathered into alumina and iron hydroxide minerals by very intense leaching of the alkali and silica (**Hutchison, 1983**). The high content of TiO_2 is recorded in the ferruginous and mottled rocks with an average up to 4.49% and 4.3% respectively. Like Al and Fe, Ti may become enriched relatively or absolutely by migration and precipitation from solution (**Migdisow, 1960**).

The high content of TiO_2 values is governed by the amount of Ti available in the source rocks and by the degree of mobilization. There are a largely parallel trend of increasing Al and Ti values in the investigated lateritic rocks. On the other hand, TiO_2 content recorded in the siliceous duricrust is (1.09%) with slightly increasing in the claystone (1.49%). However, in clayey basalt it reaches (2.54%), with slightly increasing in highly weathered basalt (3.7%), and weakly weathered basalt (3.32%). The gradual increasing of TiO_2 content from the weakly weathered basalt (3.32%) to highly weathered basalt (3.7%) followed by mottled rocks (4.31%), strongly suggest that the high concentration of the lateritic rocks with TiO_2 rather than the source basalt rocks during the different stage of weathering.

MnO high content is recorded in the weakly weathered basalt (source rock) that reaches (o.63%). However, in other varieties, it decreases. Both lateritic duricrust and siliceous duricrust have same average content (0.07%), with slightly increasing in the ferruginous rocks (0.08%) and mottled rocks, (0.09), the lowest content is obtained within claystone (0.02).

Accordingly, the behavior of MnO was accompanied by strong removal during the different stages of laterite formation.

MgO and CaO average contents show gradual decreasing from the weakly weathered basalt (source rock) to highly weathered basalt and claystone. However, MgO average, content reaches (4.46%) in the weakly basalt and (2.89%) in the claystone. On the other hand, CaO reaches (10.8%) in the weakly weathered basalt, (6.36%) in the highly weathered basalt and (3.37%) in the claystone. The lowest content of MgO is recorded in the siliceous duricrust (0.15%), whereas for CaO is recorded in the mottled rocks (0.74%). Both show an increasing from the mottled rocks to the ferruginous rocks.

Actually, MgO has value up to (0.75%) in the mottled rocks and (0.96%) in the ferruginous rocks, where CaO has value up to (0.74%) in the mottled rocks and (2.06%) in the ferruginous rocks.

Behavior of TiO_2 distribution exhibits as MgO & CaO, However, a noticeable decreasing is observed from weakly weathered basalt to highly weathered basalt and clay basalt (0.72%, 0.41% & 0.35% respectively). On the other hand, the lowest content is obtained in the mottled rocks (0.071%), however it decreases, reaches (0.36%) in the ferruginous rock, and it becomes lesser in the siliceous duricrust (0.14%) and lateritic duricrust (0.26%).

2.2. Distribution of trace elements

To show behavior and distribution of the measured trace elements, their concentration in each of the examined 8 subunits must be clearly discussed, in addition to the relationship between the source rocks and the obtained developed laterite. On the other hand, increasing and decreasing of trace element contents must be shown during decomposition of the source rock and development of laterite deposits during different stages of weathering processes. So, it is worthy to classify the examined trace elements into the following three groups:

a- Trace elements with highly connected with the basic rocks. These are Sr, Ba, V, Co, Cu, Cr and Ni.

b- Trace elements highly connected with the acidic rocks. There are Pb, Zn, Rb, Zr, Nb, Y, Mo, Nb, and Ta.

c- Radioactive elements, these are: Ga, Th, and Hf.

a- Behavior of trace elements with highly connected with the basic rocks.

Sr content in the most of the examined rock units is relatively high. However, it ranges from (89.6ppm) in the siliceous duricrust to (348ppm) in the mottled rocks. In the other hand, in the ferruginous rocks, it reaches (260ppm) and (154.8ppm) in the lateritic duricrust. Moreover, Sr content is gradually decreasing from the weakly weathered basalt (source rock), (312ppm), to claystone (210ppm). Moreover, it becomes (277.3ppm) in the highly weathered basalt and (235ppm) in the clayey basalt (Tables 27 & 28). Generally Sr concentration shows slight increasing in the different developed rocks (Laterite and related rocks), relative to the source rock (weakly weathered basalt).

Ba high content (586ppm) is recorded in the weakly weathered basalt, and low content (290ppm) in the lateritic duricrust. On the other hand, Ba content show slight decreasing in the mottled (495ppm) and ferruginous rocks (387ppm) than that of the source rock (586ppm) to indicate removing of Ba during the development of laterite deposits. The lower content is recorded in the lateritic duricrust (9oppm), while it reaches (418ppm) in the clayey basalt and (391ppm) in the clay deposits (Tables 29 & 30).

A strong enrichment of V content in the ferruginous rocks (773ppm) and mottled rocks (664ppm) may show generally stronger enriched than the source, weakly weathered basalt (160ppm) and highly weathered basalt (236ppm). Decreasing of V content from clayey basalt (296ppm) and claystone deposits (275ppm) as well as from lateritic duricrust (212ppm) to siliceous duricrust (111ppm) may reflect highly enrichment of V content during laterite formation, accompanying by slightly decreasing during formation of clay minerals (Tables 29 & 30).

Co content shows some differences as compared with V content, the highly value is recorded in the ferruginous rocks (101ppm) while the lower value (29.2ppm) in the mottled rocks. However, it shows random distribution in the other rock unit. It is noticed that the value decreases from the weakly weathered basalt (59.6ppm) to the highly weathered basalt (42.9ppm) and then increases in the clayey basalt (70.3ppm), (Tables 29 & 30).

Contents of Cu in the mottled rocks (7.88ppm) and the ferruginous rocks (23ppm) are lesser than the weakly weathered basalt (55.7ppm). The high content is found in the claystone deposits. However, the lateritic duricrust has approximately the same value of the ferruginous rocks, probably suggests the strong removal of Cu during laterite formation. According to the cross sections which plotted in the geologic map (Fig.1) and (Tables 29 & 30), the northern and southern parts of considerable laterite deposits, appear with low Cu content. The slight decreasing of Cu content in the mottled rocks and ferruginous rocks, than that in the weakly basalt, may reflect the slow removing of Cu during laterite formation.

Cr content gradually increases from the weakly weathered basalt (15.7ppm) to highly weathered basalt (49.5ppm) and clayey basalt (55,07pp). On the other hand, Cr is relatively of high value (109ppm), in the mottled rocks, and moderate value (67.5ppm) in the ferruginous rocks, but it reaches the maximum (166ppm) in the siliceous duricrust. The noticeable increasing of Cr content in the different laterite rocks units and related rock units, strongly suggests parallel concentration of Cr during formation of laterite deposits coinciding well within that has been shown of Al & Fe distribution.

Ni exhibits such as other trace elements, which occurs in obtained rock units with content lesser than in the weakly weathered basalt (source rock). However it reaches (53ppm) in the weakly weathered basalt, (12ppm) in the highly weathered basalt, (40.6ppm) in the clayey basalt and (21.7ppm) in the claystone. The content shows an increasing (45ppm) in the mottled rocks, and sudden decreasing (16.9ppm) in the ferruginous rocks, the minimum value is recorded in the siliceous duricrust (10.9ppm), while in the lateritic duricrust, it reaches (32.4ppm), (Tables 29 & 30). The distribution and concentration of Ni content may give an evidence for the irregular removing of Ni during the formation of laterite deposits.

Tables 29-30. Show the average trace elements contents of the different regolith profile units.

Table 29

	Sr	Ga	Ba	Rb	Ta	Zr	Th	Nb	Hf
Saprock (Low Weathered Basalt)	312	2	586	11.3	0.3	273	0.5	38.1	0.8
Saprolite (Highly Weathered Basalt)	277.3	0	412	6.35	0.6	210	1.0	23.7	1.2
Saprolite (Clayey Basalt)	235	3.1	418	13	0.4	887	1	81.3	1.3
Claystone	210	0	391	18.7	0.4	811	2.2	83.7	3
Mottled rocks	348	14	495	8.85	1.4	278	2.3	44	3.7
Lateritic duricrust	154.8	0	290	13.8	0	953	0	86.5	0
Ferruginous laterite	260	4.68	387	6.77	1.8	200	3.1	38.1	5
Siliceous duricrust	89.6	0	386	15.7	3.5	149	6.63	22.6	5.1

Table 30

	Y	Cr	Pb	Ni	V	Zn	Co	Cu	Mo
Saprock (Low Weathered Basalt)	21	157	7.3	53	260	141	59.6	55.7	0.29
Saprolite (Highly Weathered Basalt)	11	49.5	4.4	12	236	147	42.9	34	0.5
Saprolite (Clayey Basalt)	45.7	55.07	13.5	40.6	296	203	70.3	130	0.2
Claystone	45.2	45.4	15.1	21.7	275	59.1	53.2	31.1	1.2
Mottled rocks	27.6	109	14.7	45	664	72.3	29.2	7.88	0.8
Lateritic duricrust	44.3	23.1	12	32.4	212.2	125.1	58.3	23.5	0
Ferruginous laterite	20.8	67.5	16.6	16.9	773	47.2	101	2.1	1.38
Siliceous duricrust	17.28	166	10.4	10.9	111	30.9	62	20.1	2.2

b- Behavior of trace elements highly connected with the acidic rocks.

Pb content does not exceed (17.7ppm) in the mottled rocks, however the lower value is related to the highly weathered basalt (4.4ppm). However, in the ferruginous rocks it reaches (16.6) and (10.4ppm) in the siliceous duricrust (Tables 29 & 30). Actually, less content and random distribution of Pb content strongly suggest that Pb content cannot be considered as an effective element during laterite formation.

Rb cannot be considered as an effective element in the formation of lateritic deposits. It occurs with limited concentration that does not exceed (18.7ppm) in the claystone deposits, whereas it reaches (8.85ppm) in the mottled rocks and (6.77ppm) in the ferruginous rocks (Tables 29 & 30). This uneffective role in the formation of laterite is obtained by lower concentration of Rb content in the examined rocks.

Zn shows a gradual increasing from the weakly weathered basalt (141ppm) to clayey basalt (203ppm) passing by the highly weathered basalt (147ppm). However, it suddenly decreases in the claystone deposits (59.1ppm), followed by slight increasing in the mottled rocks (77.3ppm) and lateritic duricrust (125.1ppm) and then it decreases again in the ferruginous rocks (47.2ppm) and siliceous duricrust (30.9ppm), (Tables 29 & 30), that may reflect the irregular distribution of Zn concentration within the different rock units of lateritic deposits and related rocks.

Zr occurs with variable high content in most of the examined rock units. The maximum value (958ppm) is related to the lateritic duricrust. Both clayey basalt and claystone deposits have also relative high concentration (887ppm & 811ppm). In the mottled rocks, it reaches (278ppm) and (200ppm) in the ferruginous rocks, but it decreases to reaches (149ppm) in the siliceous duricrust (Tables 29 & 30). The given behavior of Zr concentration presumably suggests Zr preferability during the formation and development of clay mineralization, whereas the removal of Zr content has been adapted during the development of lateritic duricrust.

Mo content is ranging from (0.2 ppm) in clayey basalt to (2.2 ppm) in the siliceous duricrust. However it reaches (0.8 ppm) in the mottled rocks and (1.38 ppm) in the ferruginous rocks (Tables 29 & 30). Moreover, it is not represented in the lateritic duricrust, due to given an additional idea about MO deficiency during laterite formation.

Nb is represented by lowest value in the highly weathered basalt (1.2 ppm). However, it gradually increases from the weakly weathered basalt (38.1ppm) to the clayey basalt (81.3 ppm) and claystone deposits (83.9 ppm), then it decreases to reach (4.4 ppm) in the mottled rocks, followed by another increasing to reach (96.5ppm) in the lateritic duricrust. On the other hand, it reaches (38.1ppm) in the ferruginous rocks and (22.6 ppm) in the siliceous duricrust (Tables 29 & 30). The irregular distribution of Nb may reflect variation of the weathering action affected on the source rock during laterite formation.

Ta content is represented by low content in the most of the examined rock units. The maximum value

(3.5 ppm) is recorded in the siliceous duricrust. Moreover, it ranges from (0.3ppm) in the ferruginous rocks and (1.4ppm) in the mottled rocks (Tables 29 & 30).

Y shows a variable distribution, varying from (1.3 ppm) in the clayey basalt to (45.7ppm) in the claystone deposits. However, it is varying from (20.8ppm) in the ferruginous rocks to (27.6 ppm) in the mottled rocks, with slight increasing (45.7ppm) in the claystone deposits (Tables 29 & 30).

Generally speaking, the little concentration of rare elements (Nb, Ta, Y) beside Mo as well as their irregular distribution with noticeable values may show the unaffected factors during laterite formation.

c- Radioactive elements.

The radioactive elements are represented by Ga, Th an Hf. The elements are obtained as the rare elements, with neglected values, varying from nothing to (10ppm), so that they can be considered as unaffected element within the lateritic rocks (Tables 29 & 30).

3- Diagenesis

The diagenesis of the laterite and related rocks, are discussed by calculation of some parameters. Moreover, the palaeowethering affected on the source rock (protolith), weathered basalt and lateritic rocks (regolith) are discussed. On the other hand, the associated minerals are shown from EDX charts of scanning electron microscope (SEM).

The following chemical ratios and indices are used to show the diagenesis of the investigated rocks:

1- Al_2O_3 /TiO_2 ratio:

The value of Al_2O_3/TiO_2 ratio depends essentially upon the rock types (**Wronkiewicz and Condie, 1989**), however for the felsic rocks is generally >10 and can be >100 for the mafic and ultra mafic rocks is <20 and rarely <50 (**Byerly, 1999**). Al_2O_3/TiO_2 ratio is used as a primary indicator to infer the origin of the source (protolith) rock type. However, Al_2O_3 /TiO_2 ratio is ranging from 3 to 8 for the mafic igneous rocks, from 8 to 21 for intermediate igneous rocks, from 21 to 70 for felsic igneous rocks (**Hayashi, et.al., 1997**).

In the examined 21 cross-sections, Al_2O_3/TiO_2 suggests basic igneous rocks as beginning probable source rocks, for the weathered regolith rocks (laterite and related rock), whereas Al_2O_3/TiO_2 reaches (6.44.) However, in the saprolith rocks (weakly and highly weathered basalt and clayey basalt) it reaches (4.49), while it reaches (6.60) for the pedolith rocks (Plasmic clay, mottled zone and lateritic residuum). The given results my give an evidence for removal the mafic minerals at the upper most of the laterite section during progress of the weather action.

2- K_2O/Na_2O ratio

On the other hand, the high K_2O/Na_2O ratio favors the occurrence of illite, while the low ratio means that these sediments have originated from basic or intermediate igneous rocks (**Garrels and Christ, 1965, Weaver, 1967**).

K_2O/Na_2O ratio shows a variable variation in the different rock types. In the saprock, it varies from (0.27) in the weakly weathered basalt to (0.36) in the highly weathered basalt, followed by (0.71) in the clayey basalt, however in the pedolith it varies to (0.65) in the clay deposits, however, it increases to (3.02) in the mottled rocks, and it increases to reach (2.36) in the ferruginous rock, while it becomes (1.24) in the lateritic duricrust and more increases to (51.27) in siliceous duricrust. The irregular variation of K_2O/Na_2O ratio probably reflects the variation of leaching alkalis during formation of the laterite deposits.

3- K_2O/Al_2O_3 ratio

K_2O/Al_2O_3 ratio for saprolith rocks (weakly weathered basalt, clayey basalt and highly weathered basalt) is varying from zero to (0.15) with average (0.03). For the pedolith rocks (clay, mottled, lateritic duricrust, ferruginous rocks and siliceous duricrust) it is ranging from zero to (0.17) with average (0.08).the given similar value of saprolith and pedolith rocks, quietly reflects unique origin for the developed source rocks (Natash volcanics).

4- Chemical index of the alteration (CIA)

This index is proposed by **Nesbitt and Young, (1982**) as Al_2O_3/ $(Al_2O_3+CaO+Na_2O+K_2O)*100$. The index has been established as a general indicate of the degree of the chemical weathering in any provenance region (**Nesbitt and Young, (1982**). High values (96 - 100) indicate the intensive chemical weathering in the source area, whereas the low values (50 or less) indicate unweathered source area. The CIA can be considered as most important factor for the studied laterite and related rocks. The values of the index gradually increase from weakly weathered basalt (33.18) to highly weathered basalt (46.36) and clayey basalt (53.8), clay deposits (65.26), ferruginous rocks (88.36) and mottled rocks (91.17). Then it decreases in lateritic duricrust (56.36) and siliceous duricrust (68.37). The varies of CIA values reflect the degree of the chemical weathering and the proportionately under humid conditions, with leaching alkalis (Na^{+1}, K^{+1}) and Ca^{+2} with concentration of Al^{+3} and Fe^{+3}.

The calculated CIA values precisely show the degree of the chemical weathering that ranges from slightly weathering action along saprock (weakly weathered basalt) that had been increased upward along regolith (highly weathered basalt, clayey basalt). On the other hand, the mottled and ferruginous rocks had been affected by the higher chemical weathering accompanied often by increasing of the iron and aluminum content. However, the lateritic duricrust was affected by slightly chemical weathering action (56.36) which still has some pisolitic and nodular basalt (Tables 31-38).

The plots of CIA against Ti/Al (**Roy et al., 2008**) show different degrees of the chemical weathering affected on the investigated laterite and related rocks, varying from low to moderately weathering for saprolith rocks to highly weathering action for pedolith rocks (Fig.7).

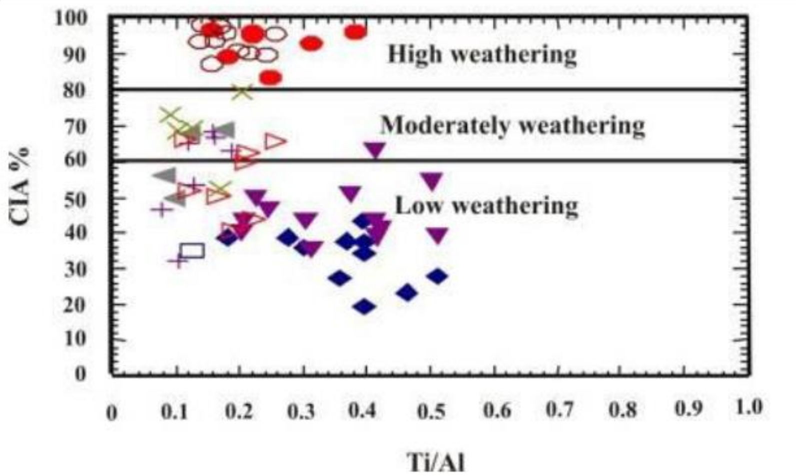

Fig.7. Plot of CIA values versus Ti/Al ratio (**Roy *et al.*, 2008**). Symbols as in Fig. (34)

5- Index of compositional variations (ICV)

ICV index is proposed by **Cox et al (1995)** as ICV = (Fe_2O_3 + K_2O + Na_2O + CaO + MgO + MnO + TiO_2) / TiO_2, whereas the high value of ICV is recorded in the lateritic duricrust that varies from 9.76 to 24.73 with an average 14.36, the low value is recorded in the mottled rocks, that ranges from 6.59 to 11.67 with an average 6.35. The noticeable variation of ICV values quietly reflects the variation of chemical composition of the investigated rock units during different stages of weathering actions (Tables 31-38).

6- Plagioclase index of alteration (PIA)

Table 31. Show some chemical parameters of the saprock (Weakly weathered basalts)

Parameters	1-9	2-5	5-2	7-5	9-6	13-8	14-6	15-3	18-6	19-5	20-5	21-6	Av.
SiO_2/ Al_2O_3	4.67	4.22	3.84	3.78	4.07	4.23	3.77	4.81	3.01	3.95	4.40	5.12	3.33
K_2O/Na_2O	0.55	0.44	0.41	0.65	0.44	0.04	0.40	0.05	0.05	0.00	0.03	0.23	0.27
K_2O/Al_2O_3	0.08	0.06	0.09	0.11	0.06	0.02	0.09	0.02	0.02	0.00	0.00	0.04	0.04
K2O/MgO	0.27	0.09	0.21	0.28	0.15	0.06	0.21	0.54	0.05	0.00	0.01	0.40	0.18
TiO_2/Al_2O_3	0.34	0.35	0.32	0.31	0.24	0.35	0.26	0.45	0.16	0.40	0.34	0.27	0.31
Al_2O_3/TiO_2	2.87	2.85	3.06	3.18	4.10	2.85	3.74	2.22	6.20	2.44	2.86	3.60	3.33
MgO/ Al_2O_3	0.32	0.68	0.44	0.39	0.42	0.33	0.44	0.05	0.51	0.42	0.49	0.11	0.38
CIW	67.87	57.97	58.97	43.79	56.28	51.07	54.02	43.45	54.59	38.96	31.13	51.47	50.79
CIW`	86.07	87.17	81.67	85.38	87.34	70.33	81.01	66.88	67.83	75.74	80.35	83.15	79.41
ICV	8.86	10.19	9.90	11.84	11.58	8.16	11.22	6	13.73	10.56	14.66	8.66	10.44
PIA	65.79	65.32	56.58	40.87	54.64	50.55	51.54	42.74	53.92	38.93	30.98	50.27	50.17
CIA	42.98	37.14	37.49	27.28	38.65	34.26	35.76	27.70	38.91	23.21	19.47	35.38	33.18
Mn*	0.35	0.58	0.10	0.68	0.49	0.29	0.08	0.50	1.03	1.01	0.85	1.03	0.58
W*	-0.28	-0.53	-0.68	-0.93	-0.69	-1.08	-0.90	-1.38	-1.29	-1.25	-1.25	-0.94	-0.93

PIA is proposed by **Nesbitt and Young, (1982)** as PIA= {(Al_2O_3 – K_2O) / ((Al_2O_3 - K_2O) + CaO* + Na_2O)} x 100. Whereas, it is used to determine the chemical weathering action, upon the regolith section.

The calculated PIA values show gradual increasing from the saprolith rock types to pedolith rock types. It ranges from (30.98 to 65.79) in weakly weathered basalt, from (56.34 to 82.14) in highly weathered basalt, (53.31-84.64) in clayey basal, from (64.99 to 97.56) in clay deposits, from (94.10 to 98.99) in mottled rock, from (43.02 to 84.49) in lateritic duricrust, from (84.75 to 98.15) in ferruginous rocks and from (70.31 to 90.59) in siliceous duricrust. Actually, the maximum values of PIA as CIA are recorded in the mottled and ferruginous rocks indicating that they represent the more acting rocks by weathering action (Tables 31-38).

7- Chemical Index of weathering (CIW)

CIW was proposed by **Nesbitt and Young,** (**1982**) as CIW = $\{Al_2O_3 / (Al_2O_3 + CaO^* + Na_2O)\}$ x 100. It represents another factor for detecting the chemical weathering subjected upon the investigated rocks, however it gradually increase from saprolith rock type (70) to pedolith rock types (90), whereas in the ferruginous and mottled rocks it reaches (98) to show high degree of weathering accompanied by leaching of alkalis and removing of silica with increasing of iron and aluminum.

Table 32. Show some chemical parameters of the saprolite (High weathered basalts)

Parameters	1-8	6-3	6-7	10-8	11-2	12-7	12-8	14-4	14-3	14-2	16-7	17-8	Average
SiO_2/ Al_2O_3	4.03	4.31	4.48	3.60	2.98	4.26	3.78	4.26	3.55	4.27	2.84	3.03	3.78
K_2O/Na_2O	0.32	0.02	2.21	0.28	0.07	0.00	0.12	0.47	0.47	0.07	0.27	0.12	0.36
K_2O/Al_2O_3	0.03	0.00	0.09	0.04	0.02	0.00	0.05	0.12	0.04	0.01	0.04	0.02	0.03
K2O/MgO	0.12	0.01	0.26	0.10	0.44	0.00	0.77	0.36	0.12	0.04	0.13	0.08	0.20
TiO_2/ Al_2O_3	0.33	0.45	0.36	0.21	0.2	0.44	0.26	0.37	0.36	0.36	0.18	0.18	0.30
Al_2O_3/TiO_2	3.01	2.21	2.72	4.62	5	2.25	3.73	2.69	2.73	2.75	5.50	5.54	3.56
MgO/ Al_2O_3	0.30	0.28	0.35	0.46	0.05	0.68	0.06	0.34	0.32	0.47	0.31	0.25	0.32
CIW	72.23	59.98	62.21	64.16	38.39	70.33	61.70	62.96	82.75	63.77	60.97	57.90	63.11
CIW`	89.61	78.74	82.46	84.96	76.71	76.12	69.81	79.17	91.92	79.49	86.27	84.23	81.62
ICV	7.87	6.80	8.55	11.50	12.13	7.08	7.30	8.79	6.95	8.62	11.45	13.34	9.19
PIA	71.46	59.85	59.85	62.98	67.89	70.31	60.39	59.77	82.14	63.32	59.90	56.34	64.51
CIA	50.83	39.14	38.81	46.43	49.75	54.19	43.55	40.73	62.93	43.56	43.39	40.12	46.11
Mn*	0.84	0.77	0.33	0.55	-0.10	0.22	-0.15	-0.19	-0.17	0.34	0.63	0.45	0.29
W*	0.30	-0.28	-0.53	-0.63	-0.45	-0.12	-0.75	-0.50	0.40	-0.52	-0.82	-0.90	-0.4

Table 33. Show some chemical parameters of the saprolite (clayey basalts)

parameters	**1-7**	**6-1**	**12-6**	**15-2**	**18-2**	**18-4**	**20-4**	**Average**
SiO_2/ Al_2O_3	2.92	3.78	2.52	2.43	3.68	3.85	1.56	**2.96**
K_2O/Na_2O	0.17	2.18	0.12	0.27	1.14	1.09	0.00	**0.71**
K_2O/Al_2O_3	0.02	0.12	0.05	0.10	0.15	0.14	0.00	**0.08**
K2O/MgO	0.05	1.19	0.43	0.74	0.72	0.56	0.09	**0.54**
TiO_2/ Al_2O_3	0.20	0.22	0.19	0.19	0.09	0.10	0.16	**0.16**
Al_2O_3/TiO_2	4.78	4.43	6.75	5.06	10	9.16	5.97	**6.59**
MgO/ Al_2O_3	0.38	0.10	0.12	0.13	0.21	0.26	0.07	**0.18**
CIW	77.99	86.30	68.75	62.14	83.83	70.74	53.49	**71.89**
CIW`	88.62	94.59	69.34	73.30	87.98	88	54.90	**79.53**
ICV	9.52	8.06	10.73	11.31	10.39	13.33	12.69	**10.86**
PIA	79.63	84.64	67.52	59.61	81.40	67.28	53.31	**70.48**
CIA	59.42	65.71	50.04	43.88	65.83	51.48	40.36	**53.81**
Mn*	0.74	-0.41	-0.46	-0.25	-0.34	-0.11	-0.37	**-0.17**
W*	0.37	0.51	0.25	-0.82	-0.04	-0.66	-0.59	**-0.59**

Table 34. Show some chemical parameters of the clay deposits

parameters	6-4	9-5	13-5	13-6	18-5	21-4	Average
SiO_2/ Al_2O_3	4.01	3.09	3.38	2.81	3.68	3.27	**3.37**
K_2O/Na_2O	2.21	0	0.01	0.02	1.21	0.48	**0.65**
K_2O/Al_2O_3	0.14	0.05	0.00	0.00	0.15	0.08	**0.07**
K2O/MgO	1.07	3.88	0.17	0.23	0.69	0.48	**1.08**
TiO_2/ Al_2O_3	0.18	0.13	0.08	0.06	0.10	0.15	**0.11**
Al_2O_3/TiO_2	5.27	7.25	11.48	14.31	9.54	6.54	**9.06**
MgO/ Al_2O_3	0.13	0.01	0.04	0.03	0.22	0.16	**0.09**
CIW	85.23	97.70	65.17	69.21	87.58	85.67	**81.76**
CIW`	93.95	100	64.68	72.52	88.53	85.66	**84.22**
ICV	7.67	7.14	15.16	12.26	9.92	8.24	**10.06**
PIA	83.19	97.56	64.99	69.01	85.58	84.61	**80.82**
CIA	62.21	86.92	49.67	56.08	67.81	68.92	**65.26**
Mn*	-0.45	-0.58	-0.95	-0.73	-0.51	-0.37	**-0.59**
W*	0.29	--	--	-0.76	0.66	--	**0.06**

Table 35. Show some chemical parameters of the mottled zone

Parameters	2-4	4-6	4-7	4-8	4-9	4-10	7-2	7-3	8-2	Average
SiO_2/ Al_2O_3	1.81	0.77	0.40	0.79	0.77	0.77	1.66	1.41	1.54	**1.10**
K_2O/Na_2O	19.8	0.05	0.21	0.53	0.03	0.03	1.45	1.16	4	**3.02**
K_2O/ Al_2O_3	0.04	0.00	0.00	0.00	0.00	0.00	0.02	0.00	0.00	**0.00**
K2O/MgO	0.60	0.01	0.75	0.07	0.02	0.02	1	0.16	0.21	**0.31**
Al_2O_3/TiO_2	4.67	6.61	14.26	6.32	5.25	5.25	5.70	8.28	7.90	**7.13**
TiO_2/Al_2O_3	0.21	0.15	0.07	0.15	0.19	0.19	0.17	0.12	0.12	**0.15**
MgO/Al_2O_3	0.07	0.02	0.00	0.03	0.03	0.03	0.02	0.03	0.00	**0.02**
CIW	98.44	98.99	98.22	97.58	94.11	94.11	98.27	96.34	99.55	**97.27**
CIW`	99.76	99.22	99.73	99.55	97.21	97.21	98.45	99.54	99.96	**98.95**
ICV	6.68	11.67	11.52	8.17	7.34	7.34	6.59	8.06	7.78	**8.35**
PIA	98.36	98.99	98.22	97.57	94.10	94.10	98.23	96.32	99.55	**97.27**
CIA	89.75	97.44	76.73	95.25	90.09	90.09	90.58	92.99	97.66	**91.17**
Mn*	-0.37	-0.76	-0.69	-0.56	-0.60	-0.60	-0.53	-0.60	-0.44	**-0.57**
W*	2.75	2.28	2.08	2.09	1.03	1.03	2.66	1.80	3.91	**2.18**

Table 36. Show some chemical parameters of the lateritic duricrust.

Parameters	16-2	16-4	16-5	16-6	17-3	17-5	19-4	Average
SiO_2/ Al_2O_3	2.89	3.53	2.87	2.86	2.29	3.4	3.05	**2.98**
K_2O/Na_2O	1.82	0.47	1.27	1	0.20	0.18	1.15	**0.87**
K_2O/ Al_2O_3	0.17	0.15	0.17	0.12	0.11	0.19	0.10	**0.14**
K2O/MgO	1.22	0.63	0.75	0.57	0.53	0.74	0.44	**0.69**
Al_2O_3/TiO_2	7.04	8.78	9.50	7.09	14.79	11.05	6.02	**9.18**
TiO_2/Al_2O_3	0.14	0.11	0.10	0.14	0.06	0.09	0.16	**0.11**
MgO/ Al_2O_3	0.14	0.24	0.23	0.21	0.20	0.26	0.22	**0.21**
CIW	85.20	70.72	83.95	84.36	62.78	48.40	85.83	**74.46**
CIW`	91.41	75.13	87.89	89.14	65.35	48.48	92.01	**78.48**
ICV	10.92	12.15	10.65	9.76	22.47	24.73	9.84	**14.36**
PIA	82.67	67.11	81.17	82.57	59.99	43.02	84.49	**71.57**
CIA	66.63	53.30	65.27	68.15	46.14	32.38	62.85	**56.38**
Mn*	-0.49	-0.29	-0.45	-0.45	-0.05	0.08	0.00	**-0.23**
W*	0.23	-0.55	0.03	0.13	-0.78	0.37	0.26	**-0.04**

Table 37. Show some chemical parameters of the ferruginous zone.

Parameters	1-4	1-5	1-6	3-7	3-8	3-9	9-3	Average
SiO_2/Al_2O_3	2.60	1.56	2.51	0.84	0.71	0.78	0.86	**1.40**
K_2O/Na_2O	3.5	9.16	3	0.25	0.33	0.11	0.2	**2.36**
K_2O/Al_2O_3	0.00	0.05	0.07	0.00	0.00	0.00	0.00	**0.01**
K2O/MgO	0.19	0.63	0.63	0.08	0.05	0.01	0.02	**0.23**
Al_2O_3/TiO_2	2.42	6.20	4.58	5.11	7.27	5.13	3.61	**4.90**
TiO_2/Al_2O_3	0.41	0.16	0.21	0.19	0.13	0.19	0.27	**0.22**
MgO/Al_2O_3	0.02	0.09	0.12	0.02	0.01	0.02	0.03	**0.04**
CIW	92.36	97.51	85.77	97.19	98.15	97.77	97.68	**95.20**
CIW`	99.85	99.36	97.46	99.11	99.71	99.62	99.55	**99.23**
ICV	7.12	13.64	7.53	16.85	8.18	10.26	7.47	**10.15**
PIA	92.32	97.36	84.75	97.18	98.15	97.77	97.68	**95.03**
CIA	56.84	88.78	71.66	94.93	96.54	95.89	92.94	**85.36**
Mn*	-0.61	-0.76	-0.76	-0.72	-0.70	-0.65	-0.57	**-0.57**
W*	2.88	2.59	1.08	2.10	2.33	2.35	2.35	**2.24**

Table 38. Show some chemical parameters of the siliceous duricrust

Parameters	3-5	3-6	4-5	9-1	9-2	10-5	10-6	Average
SiO_2/Al_2O_3	10.51	7.25	10.81	31.98	11.21	9.55	10.18	**13.07**
K_2O/Na_2O	122	76	146	13	0.92	0.27	0.71	**51.27**
K_2O/Al_2O_3	0.157	0.07	0.18	0.045	0.05	0.04	0.07	**0.08**
K2O/MgO	24.4	76	146	0.44	1.54	5	2.36	**36.53**
Al_2O_3/TiO_2	11.04	5.6	11.04	6.67	5.66	9.11	5.30	**7.77**
TiO_2/Al_2O_3	0.09	0.17	0.08	0.14	0.17	0.11	0.18	**0.13**
MgO/Al_2O_3	0.006	0.00	0.00	0.10	0.03	0.00	0.03	**0.02**
CIW	89.40	94.41	92.23	71.27	82.82	82.41	85.78	**85.47**
CIW`	99.87	99.90	99.87	99.65	94.60	85.39	90.13	**95.63**
ICV	13.07	6.33	9.41	9.18	9.12	7.53	7.94	**8.94**
PIA	87.65	93.99	90.59	70.31	82.03	81.69	84.76	**84.43**
CIA	68.37	79.50	73.15	52.37	67	69.03	69.23	**68.37**
Mn*	-0.04	0.25	-0.54	--	-0.10	-0.30	0.28	**-0.07**
W*	2.11	2.62	2.62	0.10	0.45	0.18	0.56	**1.23**

8- Al2O3 - (CaO+Na2O) - K2O (A-CN-K)

(A_CN_K) ternary molecular proportion diagram of **Nesbitt and Young (1982)** is used for the investigated rocks. The plotted samples quietly show an increasing of weathering action from saprolith rocks (source rocks) to pedolith rocks (mottled and ferruginous rocks). According to this diagram, most of saprolith samples are lying along clinopyroxene, hornblende and feldspar trend to indicate that they are related to basic igneous rocks (Natash volcanics). However, the advantage stage of the weathering (later stage) had been accompanied by development of lateritic rocks (mottled and ferruginous rocks) that are lying along plagioclase – smectite – kaolinite – gibbsite- chlorite trend (Fig.8).

Actually, the obtained lateritic rocks had been formed by action of the chemical weathering along Wadi Natash volcanics, by decomposition of the mafic minerals and increasing of kaolinitic minerals (clay) followed by leaching of alkalis and increasing of Al^{+3} and Fe^{+3} (lateritic deposits).

9- Mn* value

The calculating of Mn* value is Mn*= log [(Mn sample/Mn shales)/ (Fe sample/Fe shales)]. The values used for Mn shales and Fe shales are $600*10^{-6}$ and $4650*10^{-6}$ respectively (**Wedepohl, 1978**).

Most of saprolith samples show significant positive Mn* values (average 0.7) to suggest that they had been formed under oxic condition or nearly suboxic, where all pedolith samples had been formed under reducing condition.

10- Mineral associations

This part deals mainly with the associated minerals with the clay, mottled and ferruginous rocks, derived from the adjacent Precambrian and Phanerozoic rocks. Identification of these associated minerals are given from EDX chemical analyses using scanning electron microscope (SEM), whereas (51) chart are shown (15 for clay deposits, 16 for mottled rocks and 20 for ferruginous rocks).

Actually 22 minerals have been identified from the given charts (Figs.9-24).

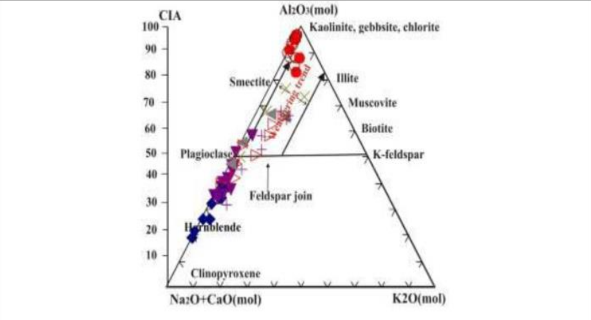

Fig.8. Al_2O_3–(CaO*+ Na_2O)–K_2O (A–CN–K) diagram for the investigated sediments (compositions as molar proportions, CaO* represents CaO of the silicate fraction only). Selected rock and mineral compositions and weathering trends (after **Nesbitt and Young, 1982**). Symbols as in Fig. (6-34).

According to the observed chemical composition. The identified minerals either metallic or non-metallic are related to the adjacent surrounding rocks.

The examined minerals (22 minerals) are classified into the following groups:

A- Minerals associated only within ferruginous rocks. These are gold (Fig.9) taenite (Ni & Fe), (Fig.10), azurite, Cu_3 $(Co_3)_2OH_2$ (Fig.11), pyrite (Fig.12), bismuth (Fig. 13) and apatite (Fig. 14).

B- Minerals associated only within mottled rocks. These are ankarite and calcite (Fig.15).

C- Minerals associated only within clay deposits, these are celesite (Fig.16) and anhydrite (Fig.17).

D- Minerals associated within mottled and ferruginous rocks. These are zincite (Fig. 18), cerussite (PbCO3) (Fig.19), siderite (Fig.16), hematite, (Figs.20) and corundum (Fig.14).

E- Minerals associated within clay and ferruginous rock. These are halite (Fig. 15) and wolframite (Fig. 21).

F- Minerals associated within all of them these are: ilmenite (Figs.17 & 22), zircon (Fig.23), barite (Fig.24), sylvite (Figs. 16, 21, & 22), and spinel (Figs. 15, 20, 21 & 22).

From above mentioned mineral associations, the following can be summarized:

1-The ferruginous rocks are characterized by association of some important metals such as gold, nickel (taenite, Ni-Fe), cupper (azurite, (Cu_3 $(Co_3)_2OH_2$), pyrite (FeS_2) and bismuth (Bi). Actually, occurring of these metals, particulars gold need more detailed field works to evaluate them.

2- The clay deposits are associated with celesite and anhydrite, as well as mottled rocks associated with ankarite and calcite of sedimentary origin, probably give an idea about their removing at the upper parts of the mainly ferruginous composition.

3- The associated minerals within both mottled and ferruginous rocks, such as zincite (ZnO), cerussite ($PbCo_3$), siderite (FeCo3) and corundum, probably reflect their quite own relationship with the laterite development.

4- The associated minerals within all of these rocks such as ilmenite, zircon, barite, sylvite and spinel may reflect that these minerals have been still preserved during different stages of the chemical weathering.

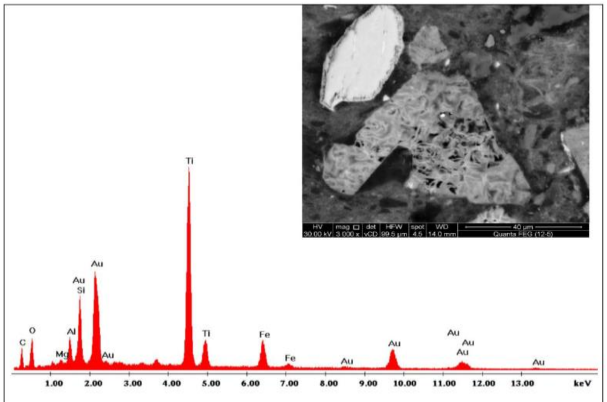

C K	12.38	31.20	0.0271	1.1214	0.1952	1.0003
O K	16.61	31.43	0.0219	1.1054	0.1190	1.0002
MgK	0.93	1.16	0.0030	1.0650	0.2997	1.0025
AlK	3.29	3.69	0.0138	1.0346	0.4052	1.0035
SiK	7.17	7.73	0.0383	1.0656	0.5002	1.0019
TiK	27.73	17.53	0.2266	0.9620	0.8416	1.0092
FeK	6.09	3.30	0.0531	0.9648	0.8883	1.0174
AuL	25.80	3.96	0.2094	0.7880	1.0302	1.0000
Total	100.00	100.00				

Fig.9. An X-ray spectrum analysis of ferruginous laterite gold grains within the rock.

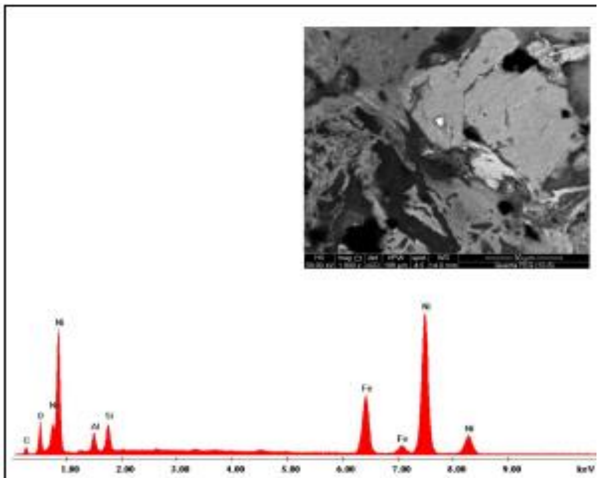

Element	Wt %	At %	K-Ratio	Z	A	F
C K	7.95	22.89	0.0126	1.1041	0.1439	1.0004
O K	9.61	20.77	0.0278	1.0883	0.2657	1.0023
AlK	4.95	6.35	0.0117	1.0186	0.2308	1.0015
SiK	6.14	7.56	0.0198	1.0492	0.3022	1.0004
FeK	14.17	8.77	0.1680	0.9481	0.9953	1.2156
NiK	57.17	33.67	0.5367	0.9668	0.9710	1.0000
Total	100.00	100.00				

Fig.10 An X-ray spectrum analysis of ferruginous laterite showing taenite mineral.

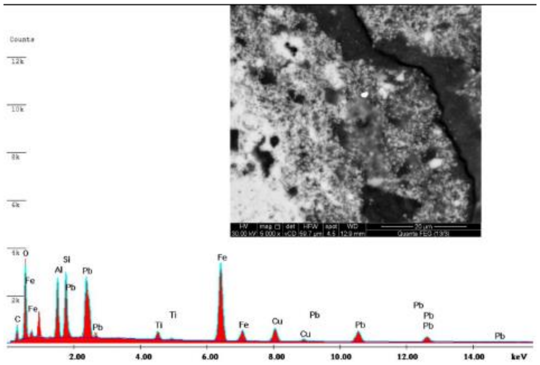

Element	Wt %	At %	K-Ratio	Z	A	F
C K	11.84	26.15	0.0219	1.0966	0.1687	1.0003
O K	25.63	42.50	0.0590	1.0810	0.2128	1.0007
AlK	8.96	8.81	0.0336	1.0120	0.3701	1.0030
SiK	9.14	8.63	0.0403	1.0423	0.4229	1.0005
TiK	1.28	0.71	0.0104	0.9385	0.8401	1.0221
FeK	18.09	8.59	0.1655	0.9420	0.9510	1.0213
CuK	4.85	2.02	0.0434	0.9181	0.9485	1.0289
PbL	20.22	2.59	0.1562	0.7483	1.0326	1.0000
Total	100.00	100.00				

Fig.11 An X-ray spectrum analysis of mottled rocks showing azurite mineral.

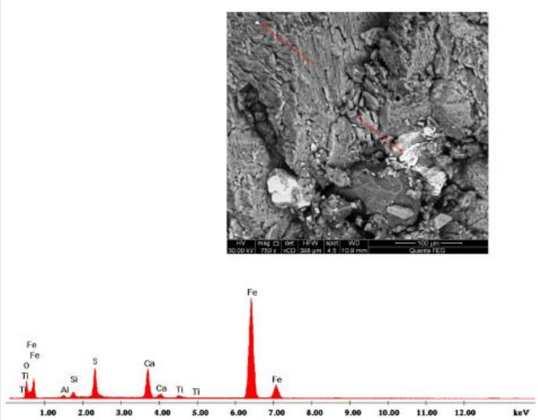

Element	Wt %	At %	K-Ratio	Z	A	F
O K	14.20	33.38	0.0352	1.0993	0.2247	1.0025
AlK	0.97	1.35	0.0026	1.0289	0.2616	1.0035
SiK	2.15	2.88	0.0082	1.0598	0.3580	1.0056
S K	8.89	10.43	0.0546	1.0528	0.5782	1.0088
CaK	8.33	7.81	0.0770	1.0426	0.8518	1.0408
TiK	0.68	0.54	0.0063	0.9530	0.8878	1.0889
FeK	64.77	43.61	0.6060	0.9574	0.9772	1.0000
Total	100.00	100.00				

Fig.12 An X-ray spectrum analysis of clay deposits showing pyrite within the rock.

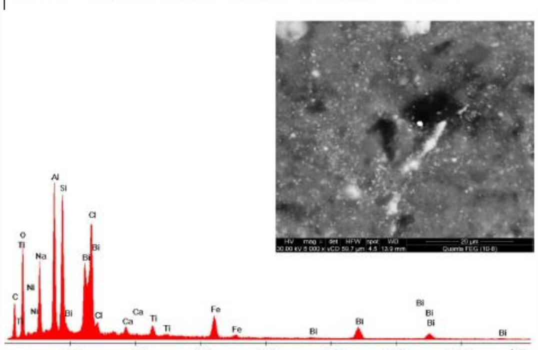

Element	Wt %	At %	K-Ratio	Z	A	F
C K	21.64	38.90	0.0319	1.0682	0.1381	1.0002
O K	21.72	29.32	0.0393	1.0531	0.1718	1.0005
NiL	0.51	0.19	0.0018	0.9396	0.3650	1.0020
NaK	7.73	7.26	0.0216	0.9891	0.2821	1.0027
AlK	10.03	8.02	0.0461	0.9861	0.4634	1.0050
SiK	10.07	7.74	0.0505	1.0158	0.4929	1.0025
ClK	7.88	4.80	0.0523	0.9669	0.6857	1.0012
CaK	0.69	0.37	0.0052	0.9947	0.7630	1.0032
TiK	1.09	0.49	0.0085	0.9103	0.8494	1.0044
FeK	3.46	1.34	0.0307	0.9150	0.9564	1.0121
BiL	15.18	1.57	0.1152	0.7218	1.0511	1.0000
Total	100.00	100.00				

Fig.13. An X-ray spectrum analysis of ferruginous zone showing bismuth within the rock.

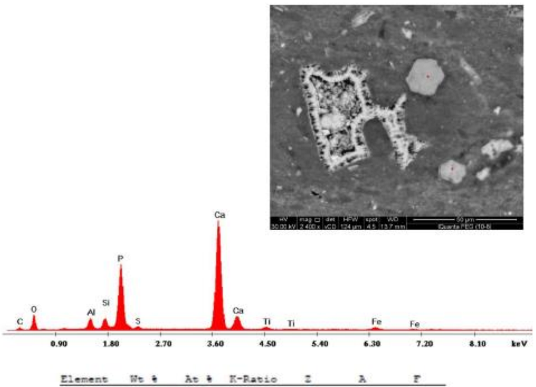

Element	Wt %	At %	K-Ratio	Z	A	F
C K	6.83	13.82	0.0114	1.0538	0.1577	1.0007
O K	27.39	41.62	0.0312	1.0388	0.1097	1.0003
AlK	3.40	3.06	0.0166	0.9728	0.4964	1.0112
SiK	3.11	2.69	0.0189	1.0021	0.5974	1.0177
P K	17.94	14.08	0.1205	0.9698	0.6845	1.0122
S K	0.73	0.55	0.0044	0.9958	0.6031	1.0179
CaK	37.37	22.67	0.3308	0.9763	0.9043	1.0024
TiK	1.29	0.66	0.0090	0.8956	0.7766	1.0018
FeK	1.94	0.85	0.0162	0.9012	0.9232	1.0000
Total	100.00	100.00				

Fig.14. An X-ray spectrum analysis of ferruginous zone of showing apatite crystals.

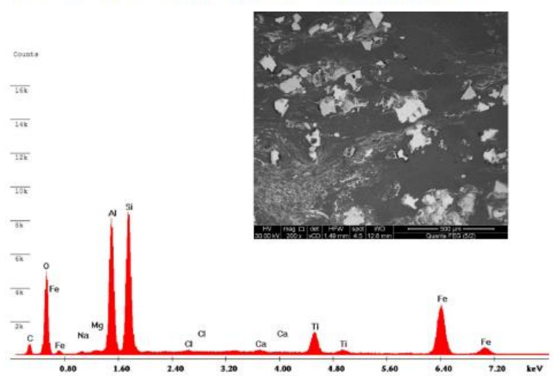

Element	Wt %	At %	K-Ratio	Z	A	F
C K	12.56	22.38	0.0176	1.0548	0.1331	1.0004
O K	29.85	39.92	0.0665	1.0399	0.2139	1.0009
NaK	0.32	0.29	0.0008	0.9768	0.2473	1.0045
MgK	0.43	0.38	0.0016	1.0024	0.3571	1.0089
AlK	16.81	13.33	0.0809	0.9740	0.4900	1.0079
SiK	21.13	16.10	0.0966	1.0033	0.4553	1.0009
ClK	0.26	0.16	0.0016	0.9551	0.6385	1.0040
CaK	0.37	0.20	0.0032	0.9754	0.8681	1.0170
TiK	3.72	1.66	0.0323	0.8954	0.9434	1.0255
FeK	14.55	5.57	0.1302	0.9013	0.9933	1.0000
Total	100.00	100.00				

Fig.15. An X-ray spectrum analysis of mottled rocks showing calcite and ankarite minerals.

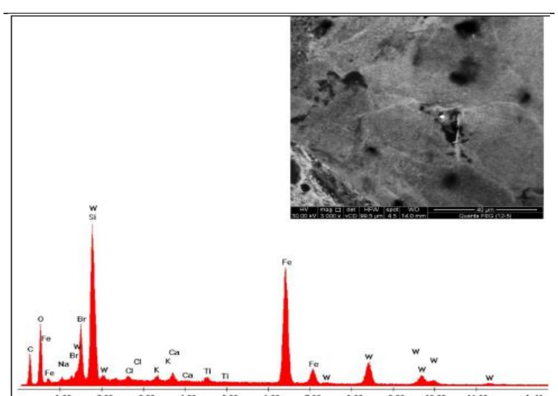

Element	Wt %	At %	K-Ratio	Z	A	F
C K	19.62	44.53	0.0361	1.1088	0.1657	1.0002
O K	16.27	27.72	0.0329	1.0930	0.1848	1.0009
NaK	0.51	0.60	0.0011	1.0263	0.2174	1.0018
BrL	10.39	3.55	0.0598	0.8909	0.6441	1.0022
SiK	7.91	7.68	0.0372	1.0538	0.4456	1.0009
ClK	0.49	0.38	0.0026	1.0026	0.5297	1.0037
K K	0.57	0.40	0.0041	1.0183	0.6952	1.0104
CaK	0.90	0.61	0.0072	1.0410	0.7627	1.0148
TiK	0.65	0.37	0.0055	0.9497	0.8630	1.0336
FeK	23.06	11.26	0.2185	0.9531	0.9636	1.0317
W L	19.62	2.91	0.1621	0.7921	1.0290	1.0134
Total	100.00	100.00				

Fig.16. An X-ray spectrum analysis of ferruginous laterite showing siderite minerals.

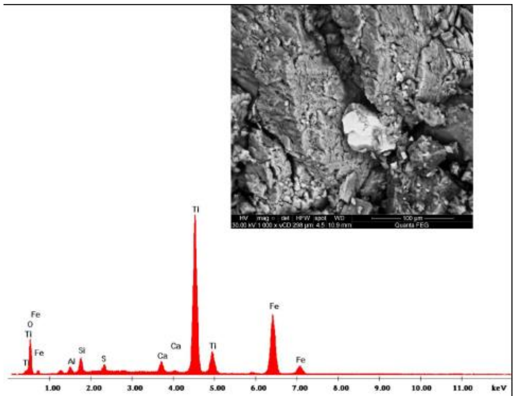

Element	Wt %	At %	K-Ratio	Z	A	F
O K	29.42	55.16	0.0402	1.0892	0.1252	1.0006
AlK	1.67	1.86	0.0054	1.0198	0.3133	1.0034
SiK	3.46	3.70	0.0153	1.0504	0.4189	1.0045
S K	1.22	1.14	0.0082	1.0437	0.6348	1.0131
CaK	1.84	1.38	0.0191	1.0287	0.9249	1.0900
TiK	36.44	22.82	0.3432	0.9419	0.9700	1.0307
FeK	25.93	13.93	0.2244	0.9470	0.9136	1.0000
Total	100.00	100.00				

Fig.17. An X-ray spectrum analysis of clay deposits showing anhydrite and ilmenite minerals within the rock.

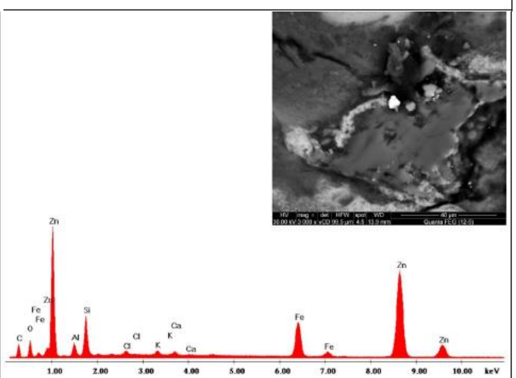

Element	Wt %	At %	K-Ratio	Z	A	F
C K	17.84	44.01	0.0258	1.1084	0.1303	1.0002
O K	6.58	12.19	0.0142	1.0926	0.1971	1.0016
AlK	3.63	3.99	0.0086	1.0228	0.2303	1.0024
SiK	9.87	10.41	0.0317	1.0535	0.3049	1.0005
ClK	0.63	0.53	0.0037	1.0024	0.5764	1.0020
K K	0.64	0.49	0.0049	1.0124	0.7552	1.0042
CaK	0.50	0.37	0.0043	1.0355	0.8188	1.0158
FeK	9.05	4.80	0.0962	0.9513	0.9878	1.1314
ZnK	51.24	23.22	0.4721	0.9283	0.9924	1.0000
Total	100.00	100.00				

Fig.18. An X-ray spectrum analysis of ferruginous laterite show Zincite minerals.

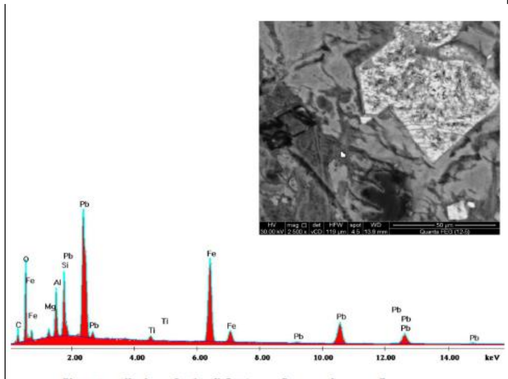

Element	Wt %	At %	K-Ratio	Z	A	F
C K	8.41	22.40	0.0166	1.1264	0.1754	1.0003
O K	21.88	43.77	0.0485	1.1103	0.1997	1.0006
MgK	1.38	1.82	0.0040	1.0695	0.2699	1.0023
AlK	5.85	6.94	0.0220	1.0389	0.3605	1.0024
SiK	7.33	8.35	0.0339	1.0700	0.4327	1.0004
TiK	0.71	0.48	0.0054	0.9697	0.7690	1.0160
FeK	18.71	10.72	0.1693	0.9712	0.9160	1.0172
PbL	35.73	5.52	0.2862	0.7792	1.0280	1.0000
Total	100.00	100.00				

Fig.19. An X-ray spectrum analysis of ferruginous laterite showing cerussite minerals.

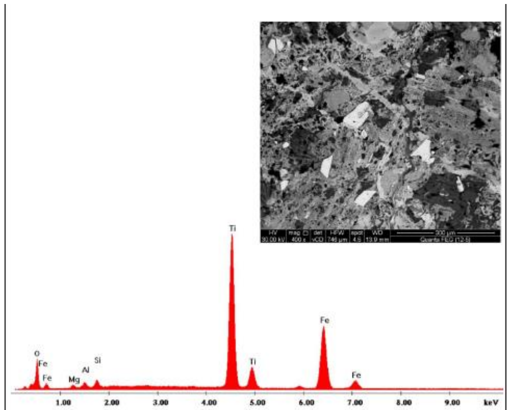

Element	Wt %	At %	K-Ratio	Z	A	F
O K	26.35	51.69	0.0366	1.0969	0.1266	1.0007
MgK	1.51	1.95	0.0035	1.0570	0.2177	1.0016
AlK	1.86	2.17	0.0058	1.0269	0.3038	1.0027
SiK	1.97	2.20	0.0085	1.0577	0.4066	1.0041
TiK	38.60	25.30	0.3733	0.9490	0.9834	1.0362
FeK	29.70	16.69	0.2596	0.9539	0.9163	1.0000
Total	100.00	100.00				

Fig.20. An X-ray spectrum analysis of ferruginous rocks showing hematite minerals.

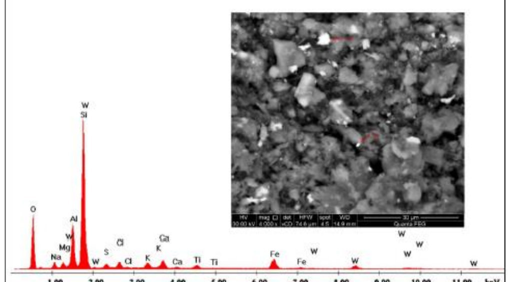

Element	Wt %	At %	K-Ratio	Z	A	F
O K	34.59	52.27	0.0795	1.0460	0.2197	1.0007
NaK	2.14	2.25	0.0061	0.9824	0.2903	1.0054
MgK	1.41	1.40	0.0057	1.0082	0.3971	1.0102
AlK	9.43	8.45	0.0469	0.9795	0.5222	1.0139
SiK	31.78	27.36	0.1757	1.0090	0.5471	1.0015
S K	1.21	0.91	0.0056	1.0026	0.4603	1.0030
ClK	1.78	1.22	0.0095	0.9604	0.5537	1.0032
K K	1.49	0.92	0.0104	0.9626	0.7210	1.0066
CaK	2.30	1.39	0.0178	0.9848	0.7822	1.0055
TiK	1.07	0.54	0.0085	0.9026	0.8732	1.0099
FeK	5.33	2.31	0.0477	0.9079	0.9698	1.0150
W L	7.46	0.98	0.0596	0.7504	1.0643	1.0000
Total	100.00	100.00				

Fig.21. An X-ray spectrum analysis of clay deposits showing wolframite within the clay minerals and beside the salt crystals.

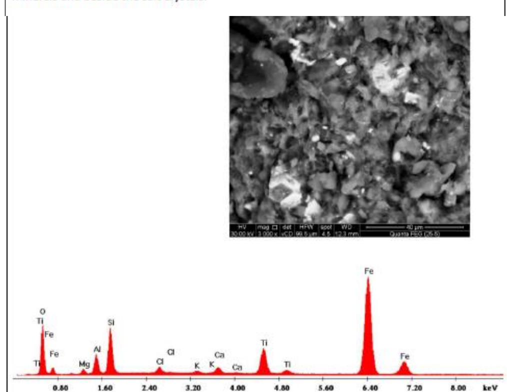

Element	Wt %	At %	K-Ratio	Z	A	F
O K	24.87	46.72	0.0647	1.0798	0.2406	1.0017
MgK	1.99	2.46	0.0046	1.0406	0.2220	1.0032
AlK	6.01	6.69	0.0187	1.0110	0.3059	1.0046
SiK	12.60	13.48	0.0502	1.0414	0.3822	1.0022
ClK	1.25	1.06	0.0080	0.9910	0.6410	1.0102
K K	0.38	0.29	0.0031	0.9969	0.8041	1.0272
CaK	1.19	0.89	0.0109	1.0198	0.8617	1.0402
TiK	6.63	4.16	0.0619	0.9238	0.9341	1.0702
FeK	45.09	24.26	0.4153	0.9388	0.9810	1.0000
Total	100.00	100.00				

Fig.22. X-ray spectrum analysis of clay deposits showing ilmenite minerals.

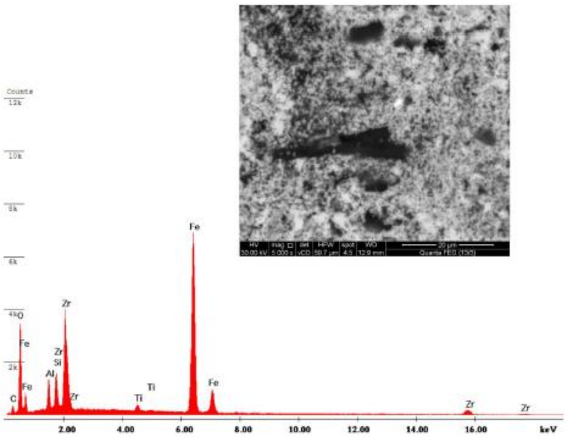

Element	Wt %	At %	K-Ratio	Z	A	F
C K	6.89	16.86	0.0116	1.1062	0.1524	1.0004
O K	25.07	46.06	0.0614	1.0906	0.2241	1.0015
AlK	4.19	4.57	0.0139	1.0209	0.3236	1.0050
SiK	4.18	4.38	0.0183	1.0516	0.4124	1.0068
TiK	0.93	0.57	0.0085	0.9447	0.9059	1.0626
FeK	42.34	22.28	0.3954	0.9493	0.9839	1.0000
ZrK	16.39	5.28	0.1391	0.8509	0.9973	1.0000
Total	100.00	100.00				

Fig.23, An X-ray spectrum analysis of mottled rocks showing zircon minerals.

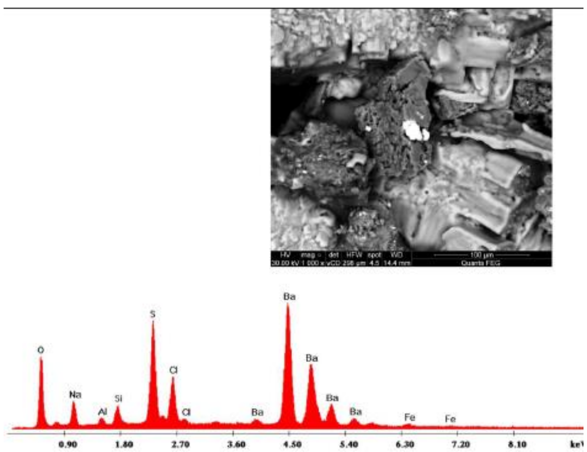

Element	Wt %	At %	K-Ratio	Z	A	F
O K	17.10	43.18	0.0496	1.1480	0.2526	1.0002
NaK	6.43	11.30	0.0126	1.0777	0.1818	1.0014
AlK	1.47	2.20	0.0040	1.0741	0.2497	1.0047
SiK	3.07	4.41	0.0112	1.1062	0.3282	1.0073
S K	12.70	16.01	0.0729	1.0986	0.5168	1.0116
ClK	6.16	7.02	0.0353	1.0521	0.5379	1.0131
BaL	52.48	15.44	0.4584	0.8607	1.0144	1.0004
FeK	0.60	0.43	0.0046	1.0048	0.8018	1.0000
Total	100.00	100.00				

Fig.24. An X-ray spectrum analysis of clay deposits showing sylvite minerals.

Conclusion

Study of the geochemical behavior of the major oxides indicated that SiO_2, Al_2O_3, F_2O_3, Na_2O_3 and K_2O represent the main restricted factor laterite occurrence and development. A direct relationship between SiO_2 distribution and intensity of weathering action is observed.

During the early stage of diagenesis, enrichment of silica is reciprocal with these oxides. Chemical, mineralogical relation took place during weathering of saprolith and pedolith according to the following steps: **a)** Kaolinitization of alumino-silicate minerals, **b)** Hematization of Fe-bearing minerals, **c)** Formation of hydroxide minerals from kaolinite or directly from feldspar through in congruent dissolution, **d)** Congruent dissolution of kaolinite minerals, **e)** Dissolution of quartz.

Generally the distribution of these five oxides (SiO_2, Al_2O_3, F_2O_3, Na_2O_3 and K_2O) proved that the investigated laterite deposits had been done in the upland area, predominantly of residual origin, under free leaching conditions. Actually, the minerals of the iron oxides by very intense leaching of alkalis and silica. Moreover, distribution of the trace elements, proved the investigated laterite have been related to basic rocks.

Calculation of chemical index of alteration (CIA), index of compositional variation (ICV), plagioclase index of alteration (PIA) and chemical index of weathering action (CIW), reflected the degree of chemical weathering, proportionally under humid conditions, whereas the mottled and ferruginous rocks represent the more acting rocks. Usually the high degree of chemical weathering action, are accompanied by leaching of alkalis and removing of silica. Actually the investigated laterite deposits had been formed by chemical weathering action of Natash volcanics and decomposition of the mafic minerals, accompanied by increasing kaolin and increasing of Al^{+3} and Fe^{+3} minerals.

Identification of the associated minerals of the laterite deposits, from EDX charts from EDX charts of scanning electron showing the following features.

1 -The ferruginous rocks are characterized by association of some important metals such as gold, nickel (taenite, Ni-Fe), cupper (azurite, ($Cu_3(Co_3)_2OH_2$), pyrite (FeS_2) and bismuth (Bi). Actually, occurring of these metals, particulars gold need more detailed field works to evaluate them.

2- The clay deposits are associated with celesite and anhydrite, as well as mottled rocks associated with ankarite and calcite of sedimentary origin, about their removing at the upper parts of the mainly ferruginous composition.

3- Both the rocks, such as zincite (ZnO), cerussite ($PbCo_3$), siderite (FeCo3) and corundum Al^2O^3, to reflect their own relationship with laterite development.

4- Most all rock units of laterite deposits and related rocks are associated ilmenite, zircon, barite, sylvite and spinel indicating that may have been still preserved during different stages of the chemical weathering.

References

1. Byerly, G.R., 1999. Komatiites of the Mendon Formation: late-stage ultramafic volcanism in the Barberton Greenstone Belt. Geol. Soc. Am. Spec. 329, p189–211.
2. Cox, P.A., 1995. The elements on Earth. Inorganic chemistry in the environment. Oxford University press, Inc., New York.
3. Dury, G.H., 1969. Perspectives on geomorphic processes. Washington: Association of American Geographers, 1969. 56.
4. Garrels, R.M., Christ, C.L., 1965. Solution, minerals and equilibria, Harper and Row Pub., New York, p450.
5. Grubb, P. I., 1973: High level and low level bauxitization: a criterion for classification, Mineral Sci. Eng. Vol.5, 219-231pp.
6. Hayashi K, Fujisawa H, Holland H, Ohmoto H (1997). Geochemistry of ～1.9 Ga sedimentary rocks from northeastern Labrador, Canada. Geochim Cosmochim Acta 61(19):4115–4137.
7. Hutchison, C.S.1983. Economic deposits and their tectonic setting. The Macmillan press LTD, London and Basingstake, 365p.
8. MacFarlane, M.J., 1983. Laterites. In: Goudie, A.S., Pye, K. (eds.). Chemical Sediments and Geomorphology: precipitates and residua in the near-surface environment. London: Academic Press, p. 7-58.
9. Migsisow, A. a., 1960. On the other titanium – aluminum ratio in sedimentary rocks, geochemistry 2:178-184).
10. Nesbitt, H.W., G.M. Young., 1982. Early Proterozoic climates and plate motions inferred from major element chemistry of lutites. Nature. 299, p715-717.
11. Roy PD, Caballero M, Lozano R, Smykatz-Kloss W (2008). Geochemistry of Late Quaternary sediments from Tecocomulco lake, central Mexico: implication to chemical weathering and provenance. Chemie der Erde-Geochemistry 68:383–393.
12. Valeton, I., 1972. Bauxites, Elsevier publishing company, Amesterdam, London, Newyork. 225p, Hutchiso, C. S. 1983: Economic deposits and their tectonic setting. The Macmillan press LTD. London and Basings toke, 365p.
13. Weaver, C.E., 1967. Potassium, illite and the ocean. Geochim. Cosmochim. Acta., 31 p281-296.
14. Wedepohl, K.H., 1978. Manganese: Abundance in Common Sediments and Sedimentary Rocks [M]. pp.1−17. Handbook of Geochemistry: Springer Berlin.
15. Wronkiewicz, D.J., Condie, K.C., 1987. Geochemistry and mineralogy of sediments from the Ventersdorp and Transvaal Supergroups, South Africa: Cratonic evolution during the early Proterozoic: Geochimica et Cosmochimica Acta, 54(2), p343-354.

8/23/2017